High Energy Diffraction Microscopy at Sector 1:
An Inside View of Materials' Responses

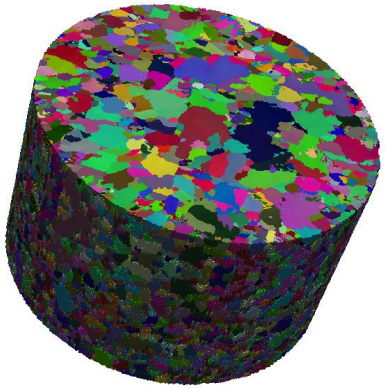

Bob Suter (suter@cmu.edu)

Carnegie Mellon University Physics

DEPARTMENT OF MATERIALS SCIENCE AND ENGINEERING

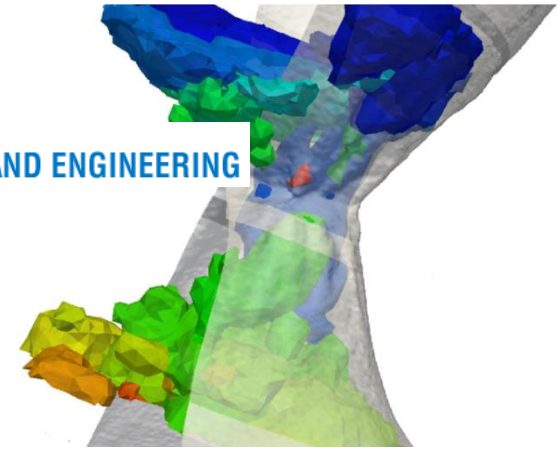

Thanks to:

CMU graduate students

SF Li, J Lind, CM Hefferan

R Pokharel, S Maddali,

X Tan, D Menasche

Sector 1 staff

[U Lienert], J Almer, P. Kenesei

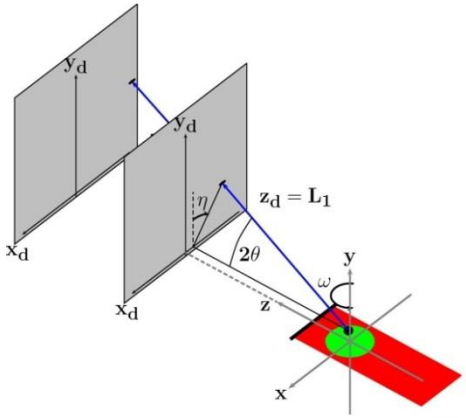

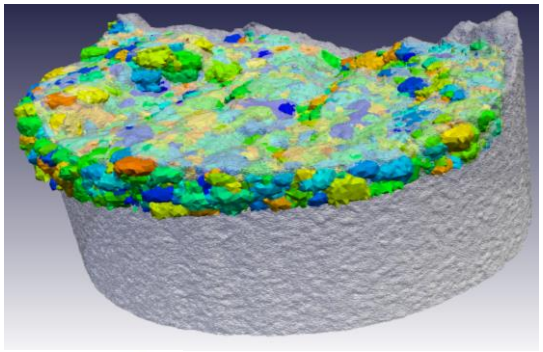

2014 Neutron & X-ray School

Underlying Motivation

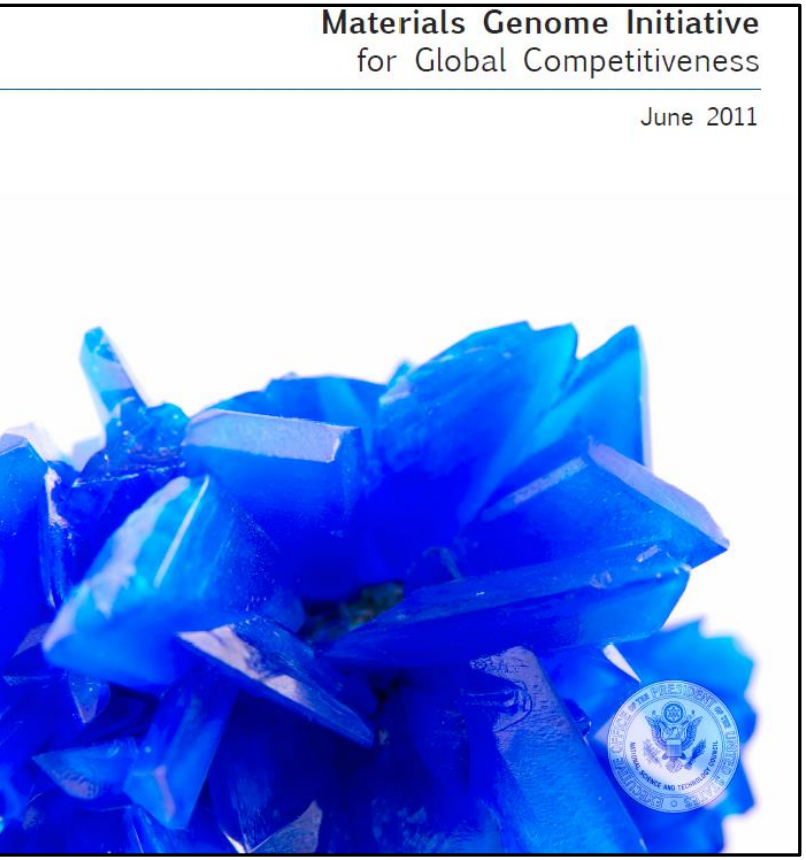

"At present, the time frame for incorporating new classes of materials into applications is remarkably long… 10 to 20 years…"

"…experiments could potentially be performed virtually with powerful and accurate computational tools, but that level of accuracy in such simulations does not yet exist."

Mesoscale experimental data that track responses in 3D under realistic conditions is urgently needed. (RMS)

High Energy X-rays: > 50 keV

- **Penetrate millimeter dimensions across much of the Periodic Table**

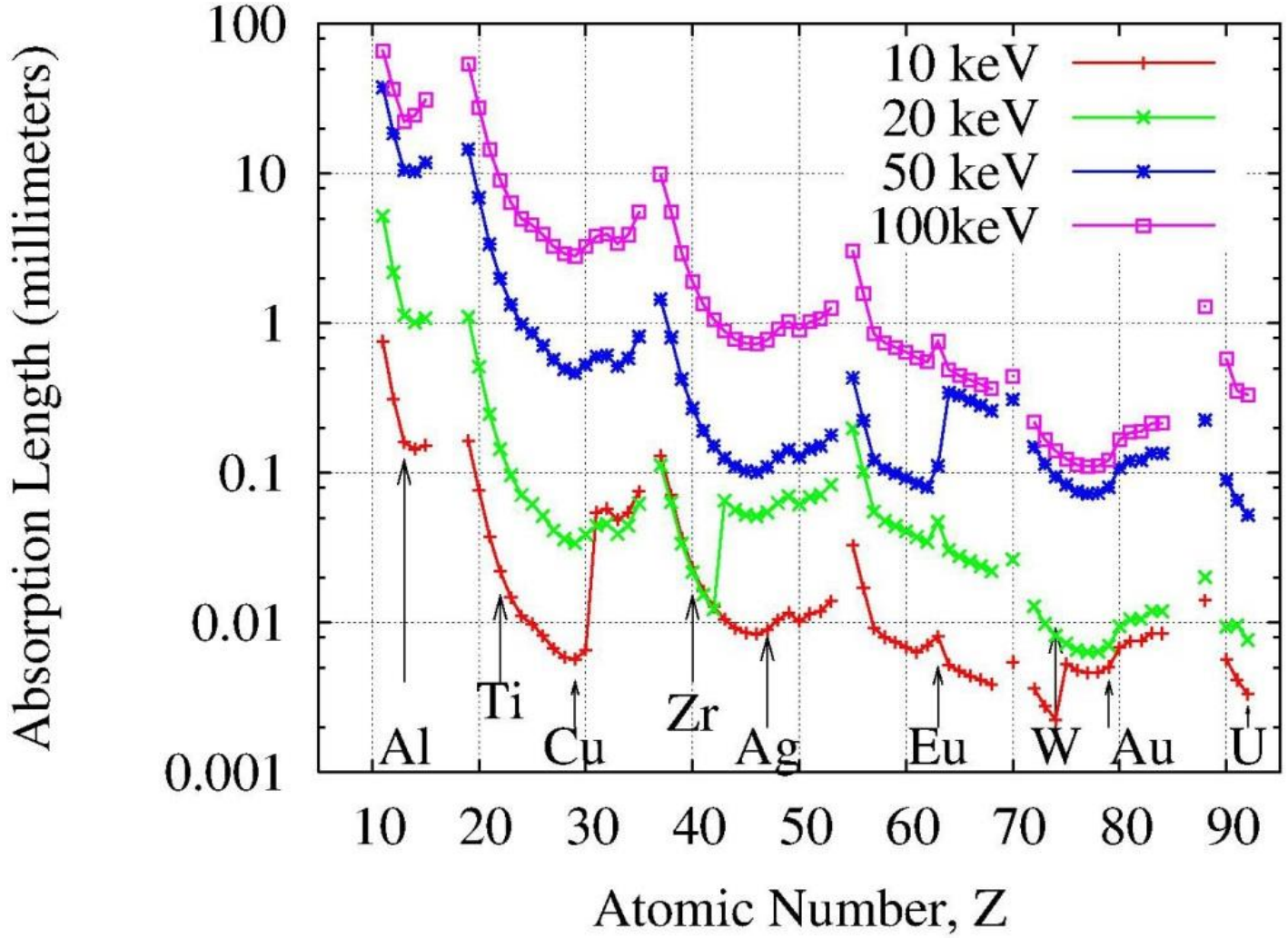

Advanced Photon Source: Spectral Range to 100 keV

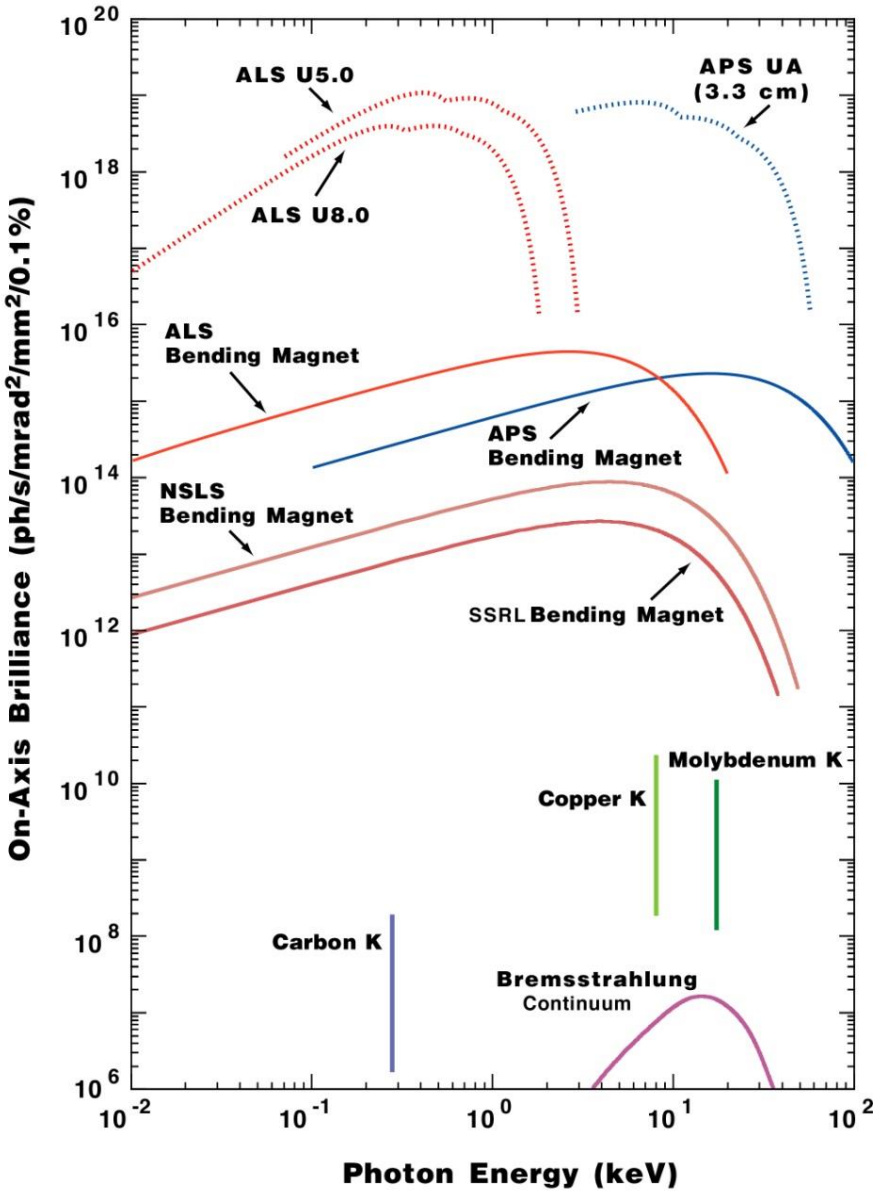

Elastic scattering of waves: kinematics

$$|\mathbf{k}_i| = |\mathbf{k}_f| = 2\pi/\lambda$$

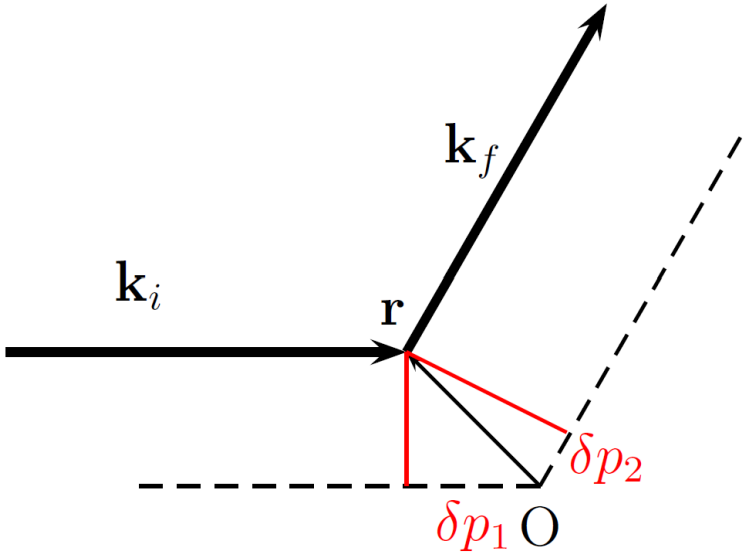

$$\Delta p = |\delta p_1| + |\delta p_2| = -\hat{k}_i \cdot \mathbf{r} + \hat{k}_f \cdot \mathbf{r} = (\hat{k}_f - \hat{k}_i) \cdot \mathbf{r}$$

$$\Delta\phi = 2\pi \frac{\Delta p}{\lambda} = (\mathbf{k}_f - \mathbf{k}_i) \cdot \mathbf{r} = \mathbf{Q} \cdot \mathbf{r}$$

Elastic scattering of waves: kinematics

$$\mathbf{Q} = \mathbf{k}_f - \mathbf{k}_i$$

Wavevector transfer or Momentum transfer

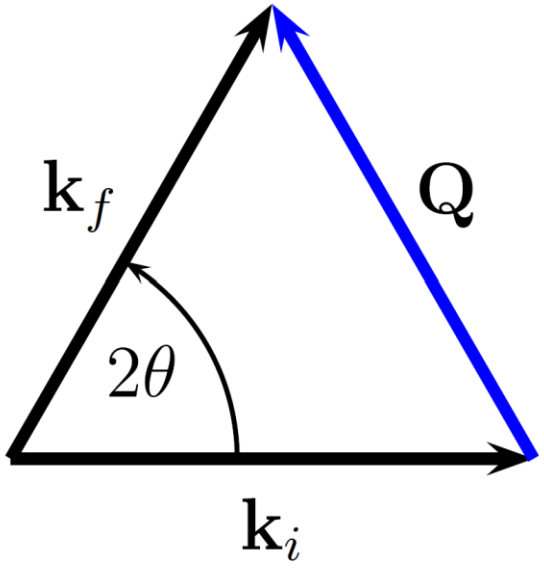

$$|\mathbf{Q}| = 2k \sin\theta$$

Born Approximation

$$A(\mathbf{Q}) = \int_{V_c} d^3\mathbf{r}\ \rho(\mathbf{r})\ e^{i\mathbf{Q}\cdot\mathbf{r}}$$

3D Fourier transform of scattering density

Bragg scattering: wavefront development

Thanks to Joel Bernier (LLNL)

[External movie file]

Crystal/Bragg scattering:

$$n \lambda = 2 d \sin \theta$$

or

$$Q = G_{hkl}$$

Born Approximation: effect of defect content on intensities

$$A(\mathbf{Q}) = \int_{V_c} d^3\mathbf{r}\ \rho(\mathbf{r})\ e^{i\mathbf{Q}\cdot\mathbf{r}}$$

3D Fourier transform of scattering density

$$\begin{aligned} A(\mathbf{Q}) &= \int_{L_\parallel} dr_\parallel \int_{a_\perp} d^2 r_\perp\ \rho(\mathbf{r})\ e^{iQr_\parallel} \\ &= a_\perp \int_{L_\parallel} dr_\parallel\ \bar{\rho}(r_\parallel)\ e^{iQr_\parallel}, \end{aligned}$$

1D Fourier transform of laterally averaged scattering density

Defect content yields thermal-like smoothing of laterally averaged density: anisotropic intensity reduction

Can this be spatially resolved?

Bragg scattering: Rotating Crystal & Area Detector

Thanks to Joel Bernier (LLNL)

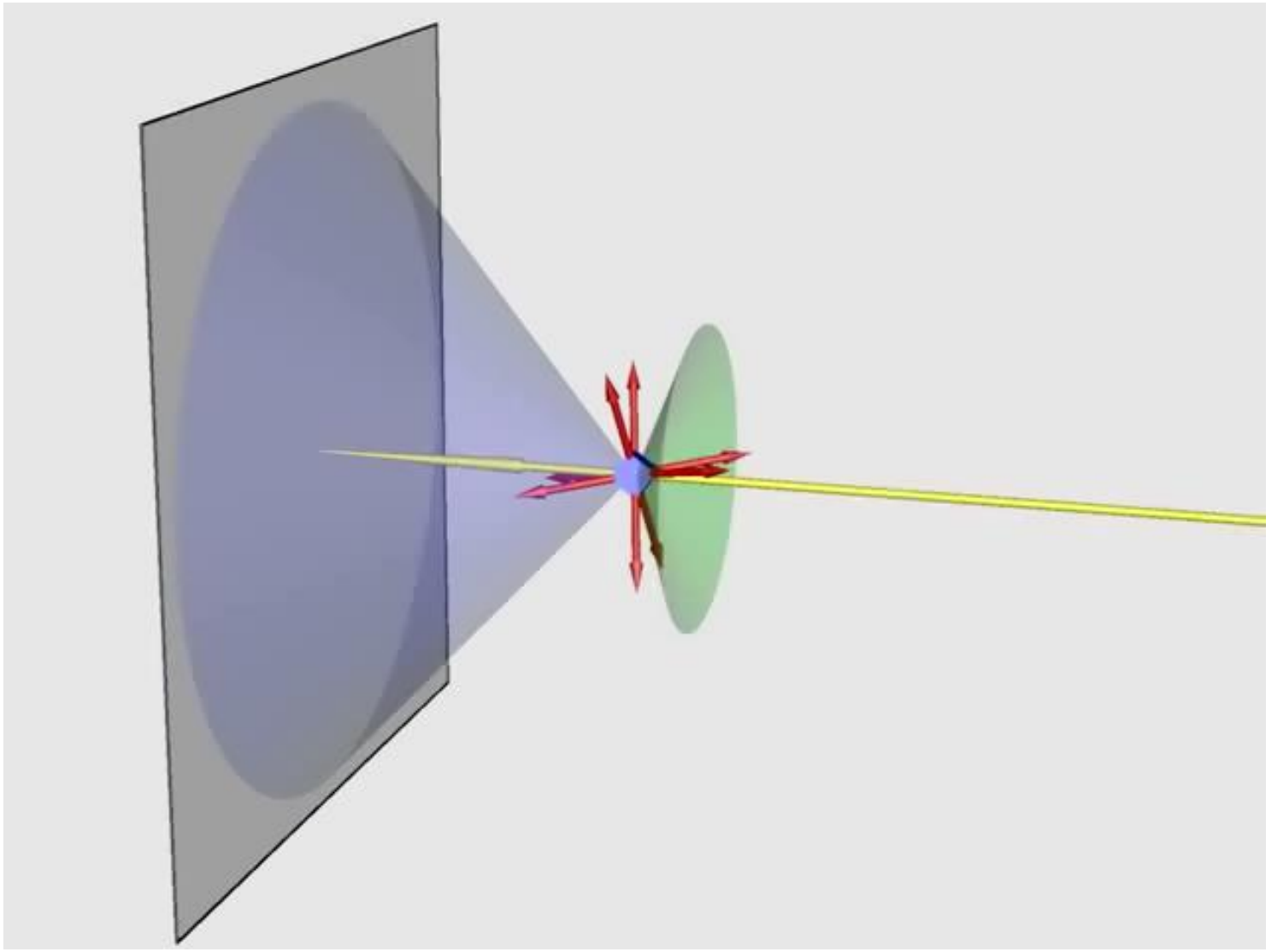

Small beam limit of powder diffraction: polycrystals

- Powder approximation: all orientations are in the beam
  - All diffraction, all the time
  - Debye-Sherrer rings on area detector
  - Intensities proportional to {hkl} multiplicities

- Polycrystal scattering
  - Solid materials with crystalline ‘grains’
  - All orientations but typically with ‘texture’
    - Non-uniform orientation distributions
    - Due to processing: rolling, drawing, etc.

- Small beams
  - Illuminate small number of grains
  - Isolate scattering from individual grains
  - Single crystal probe but in complex environment

Bragg Condition

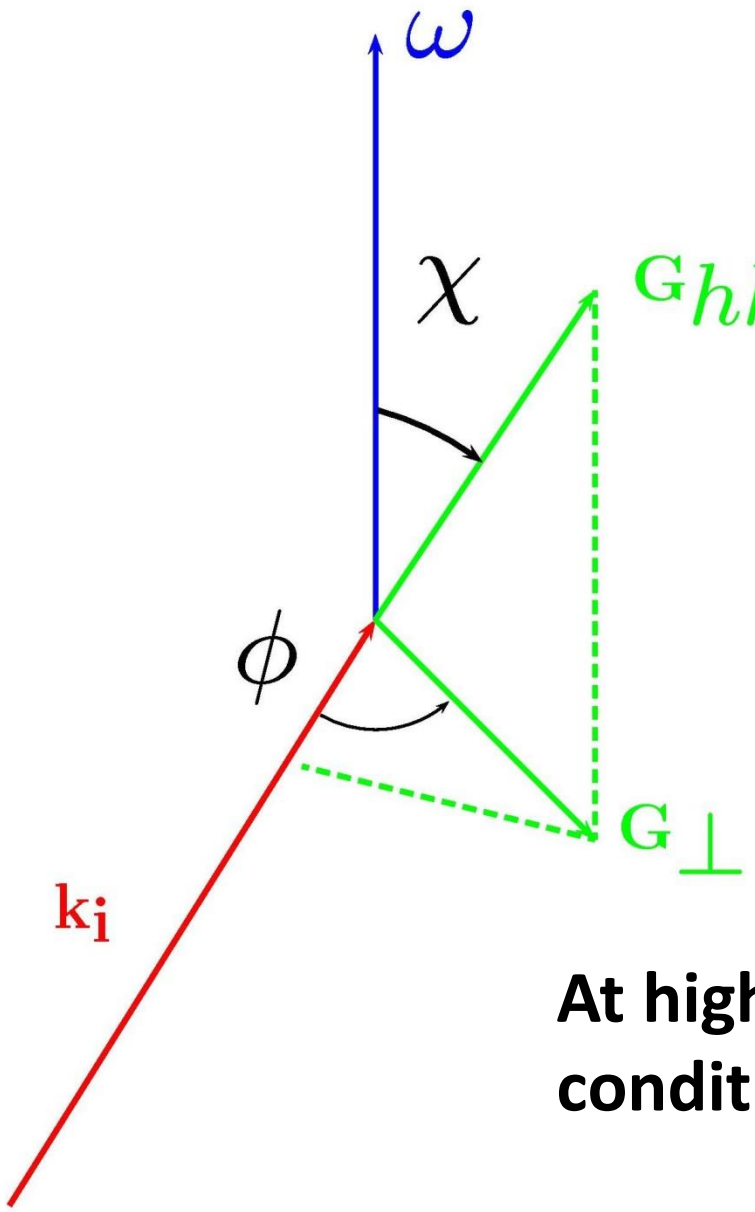

$$\mathrm{G}_{hkl} = 2k \sin\theta$$

$$\hat{\mathrm{k}}_i \cdot \hat{\mathrm{G}}_{hkl} = -\frac{|\mathrm{G}_{hkl}|}{2k}$$

$$\sin\chi \ \cos\phi = -\sin\theta$$

$$\boxed{\chi > \theta \text{ is visible}}$$

At high energies, θ's are small and this condition is not restrictive

Number of Bragg peaks over 180 degrees

$$Q_{max} = 2k \sin\theta_{max}$$

$$2k[\text{Å}^{-1}] = \frac{4\pi}{\lambda[\text{Å}]} \approx E[keV]$$

1.013

$$\text{Volume Probed} \approx \frac{4\pi}{3} Q_{max}^3$$

$$\text{Density of Bragg points} \sim \frac{V_{prim}}{(2\pi)^3}$$

$$\boxed{\text{Number of peaks} = N_{peak} \sim \frac{4}{(2\pi)^3} Q_{max}^3 \, V_{prim}}$$

Number of Bragg peaks over 180 degrees

Example: Aluminum

Near-field: $\boxed{Q_z > 0}$

$$2\theta_{max} \sim \tan^{-1}\left(\frac{3\text{mm}}{7\text{mm}}\right) = 25^\circ$$

$$Q_{max} \sim 50 \sin 12.5^\circ \approx 10\text{Å}^{-1}$$

$$N_{peak}^{Al} \approx \frac{2}{(2\pi)^3} (10\text{Å}^{-1})^3 \, 16\text{Å}^3 = \textcircled{129}$$

Number of Bragg peaks over 180 degrees

Example: Aluminum

Far-field:

$$2\theta_{max} \sim \tan^{-1}\left(\frac{0.2\text{m}}{1\text{m}}\right) = 11^\circ$$

$$Q_{max} \sim 50 \sin 5.5^\circ \approx 5\text{Å}^{-1}$$

$$N_{peak}^{Al} \approx \frac{4}{(2\pi)^3} (5\text{Å}^{-1})^3 \, 16\text{Å}^3 = 32$$

$\{111\}, \{200\}, \{220\}$: 26 peaks, $Q_{max} = 4.4\text{Å}^{-1}$.

High Energy X-rays: > 50 keV

- Penetrate millimeter dimensions
- Bragg diffraction at small angles
- Large reciprocal space coverage with small area detector and one rotation

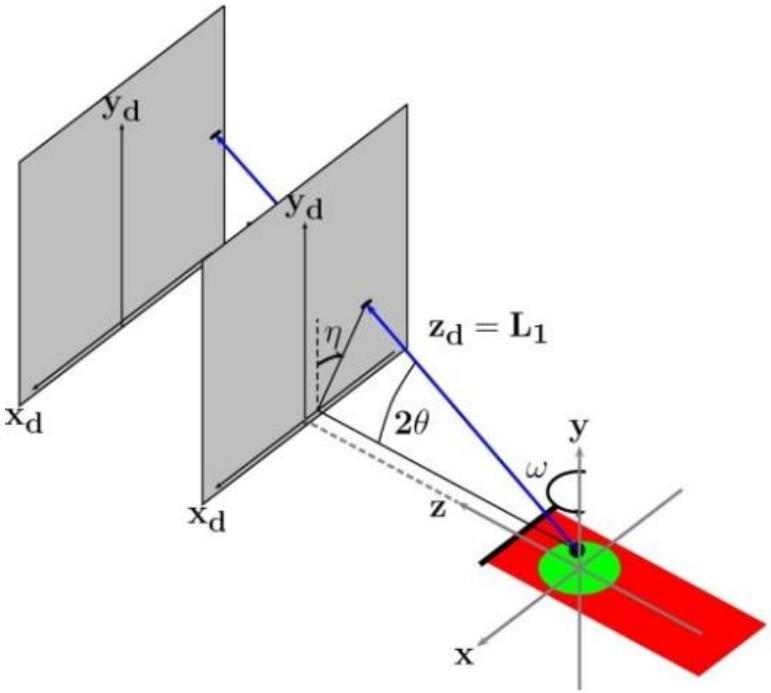

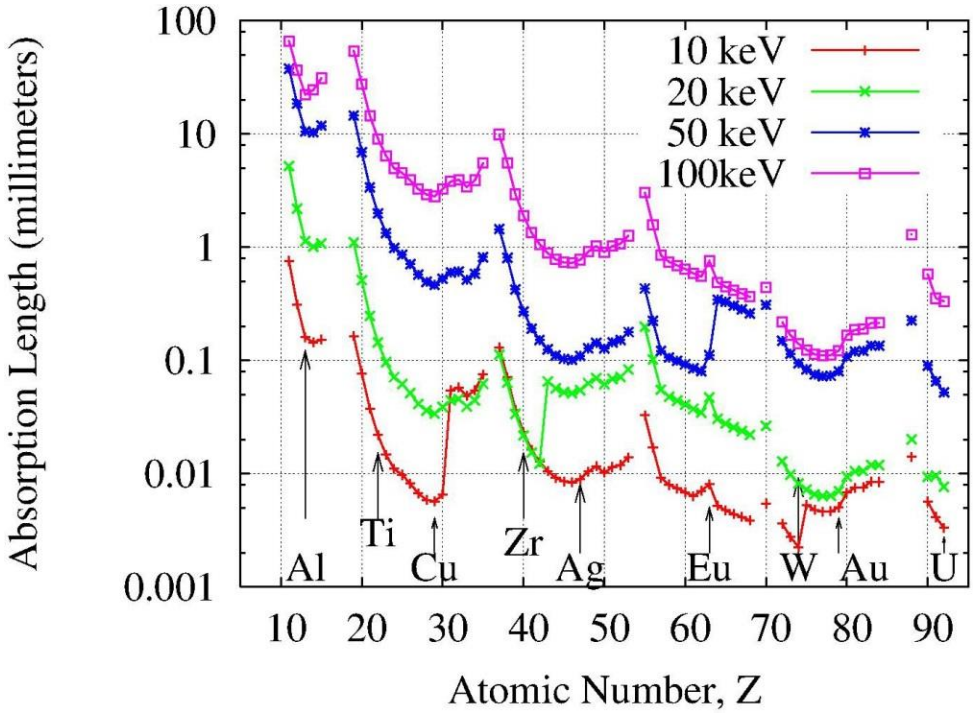

Near-field HEDM: Crystal Orientation Field Measurement

Image diffracted beams from planar grain cross-sections

APS 1-ID

- Monochromatic x-rays (> 50keV)
- 1 μm beam height
- 1 - 2 mm beam width
- 1.5 μm detector pixels (2k x 2k)
- L = 4 – 15 mm
- Air bearing rotation stage
- 0.05 < δω < 1 degree
- Δω = 180 degrees
- ~80 – 150 Braggs per orientation

- Spatial resolution: ~2 μm
- Orientation resolution: < 0.1 degree
- ~4 layer / hour measurement
- ~100 layers per volume

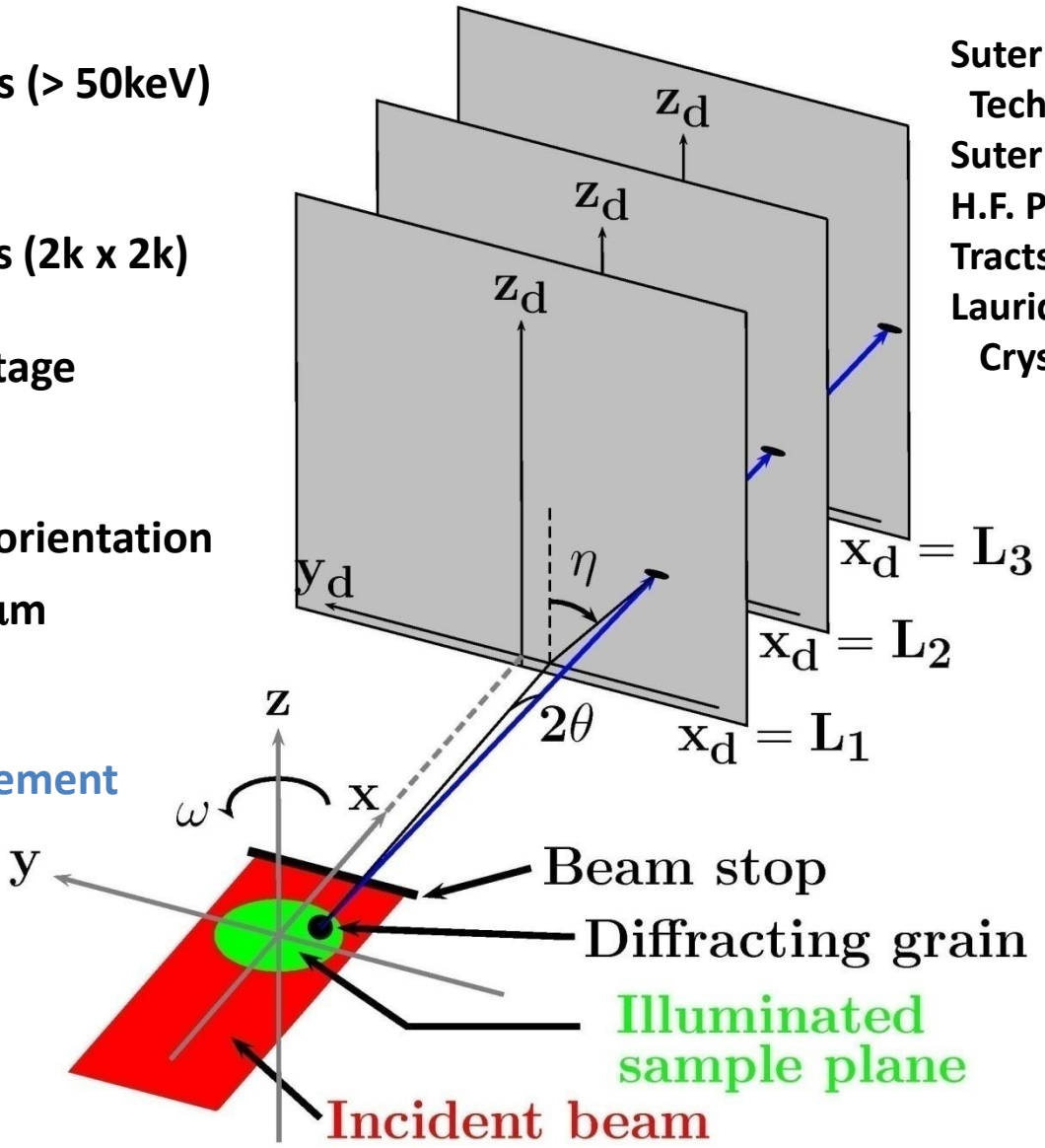

Suter et al, Eng Mat & Tech 2007

Suter et al, RSI 2006

H.F. Poulsen, Springer Tracts, 2004

Lauridsen et al, Appl Cryst 2001

Detector Image: Single Crystal Grains

- One of 180 in 180 deg
- One of 360 per layer
- One of ~ 36,000 per volume
- 288 GB per volume
- ~3.6M diffraction spots

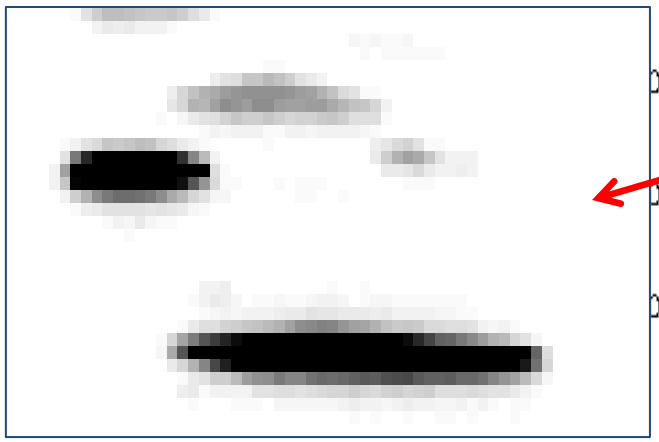

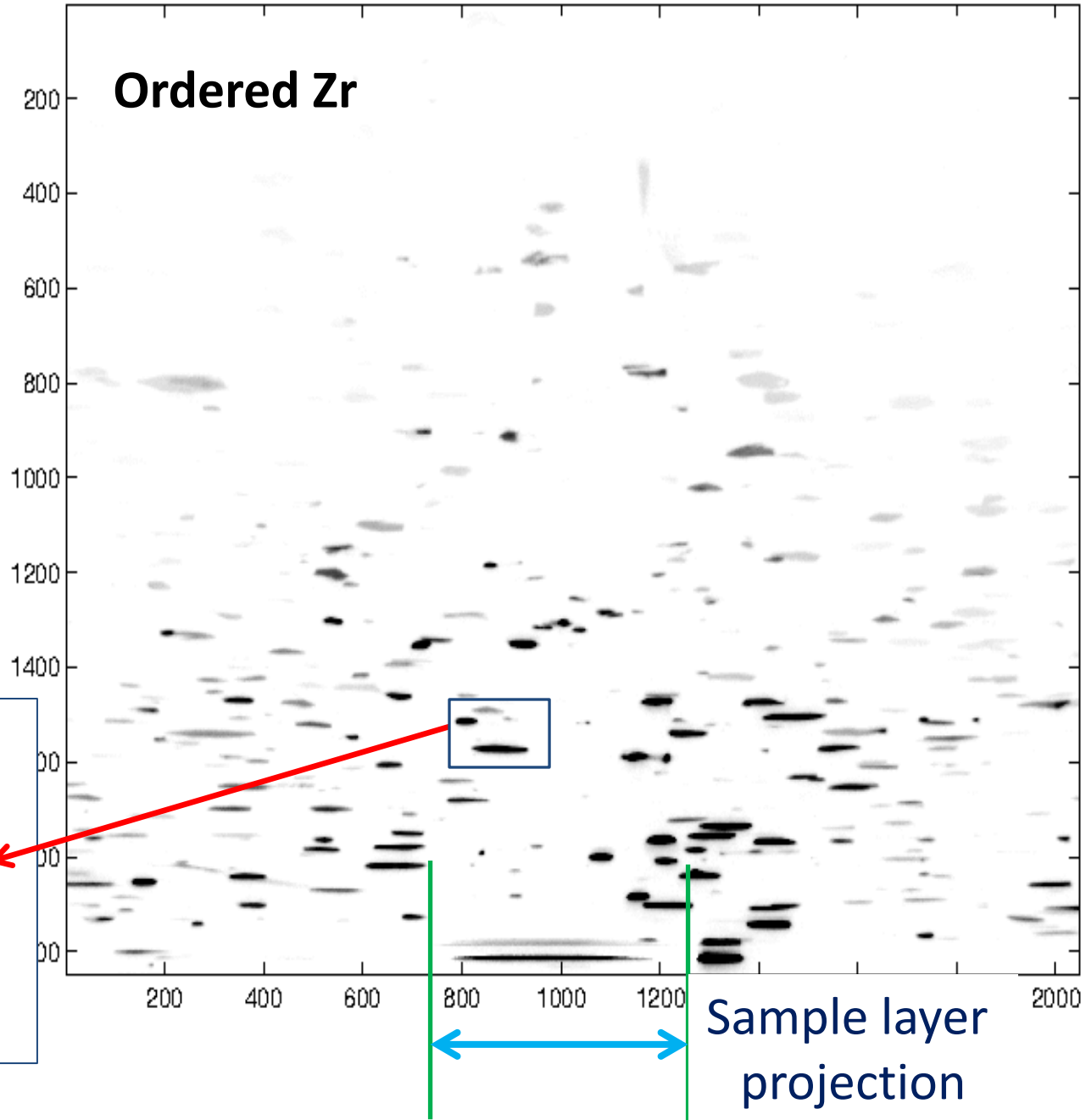

nf-HEDM: Forward Modeling Reconstruction

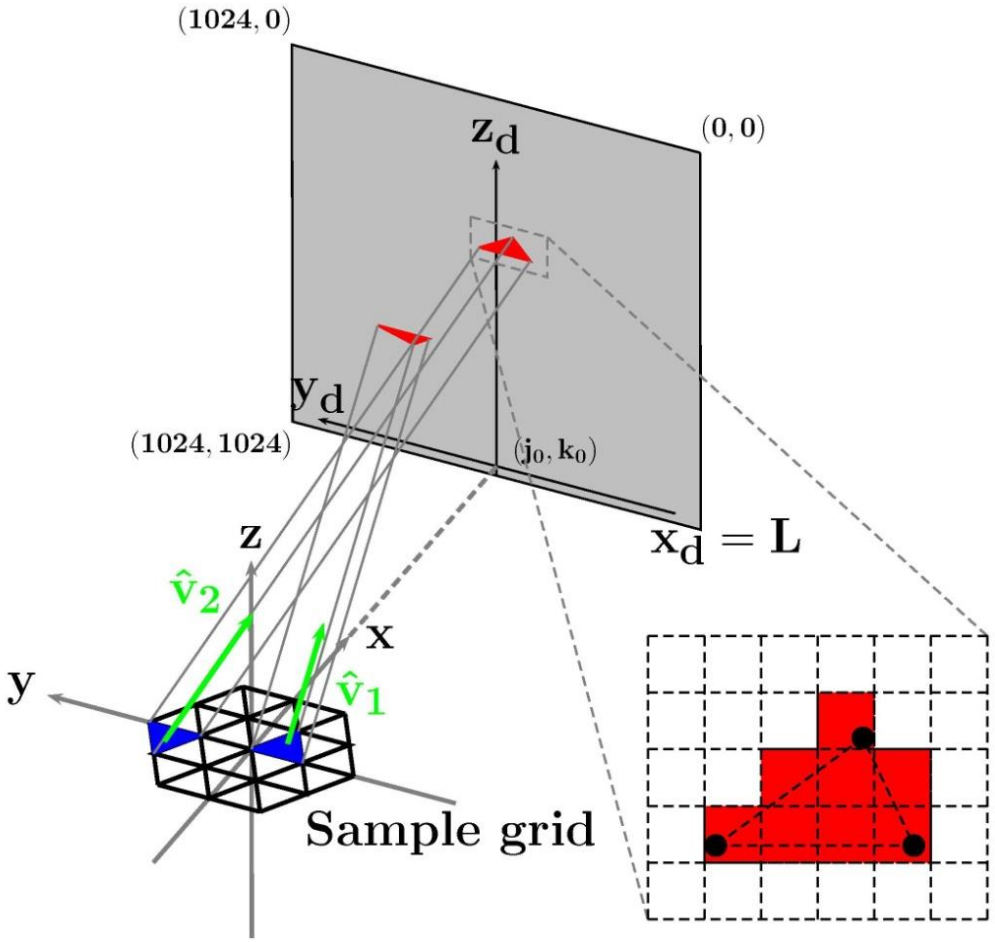

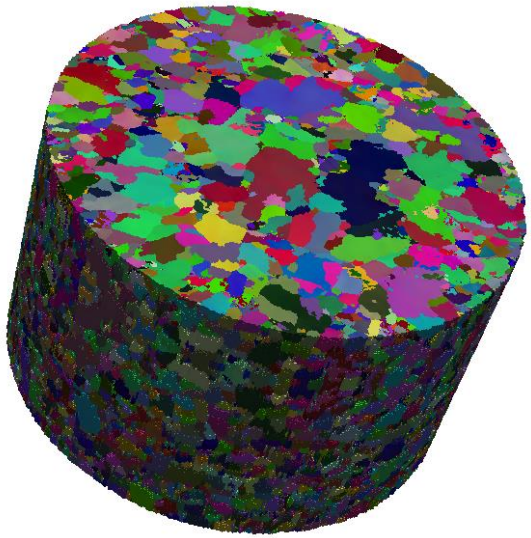

Copper: 0.4 mm³

- **Computer simulation replicates experiment**
- **~10^5 voxels/layer**
- **> 10^7 orientations resolved per voxel**
- **~100 layers**
- **Highly parallel processing:**
  CMU, APS clusters, NSF/XSEDE
- **Shortcuts:**
  - **Hierarchical search**
  - **"Growth" of found orientations**
  - **Input from far-field measurements**

Li & Suter, J. Appl. Cryst. 2013
Suter et al, RSI 2006

Confidence metric

C = fraction of simulated peaks overlapping experimental peaks

- Relative measure, not an absolute metric
- Reduction at grain boundaries/edges: extrapolating voxel scattering to edges of reduced experimental diffraction spots
- Reduction in deformed materials: loss of high Q scattering

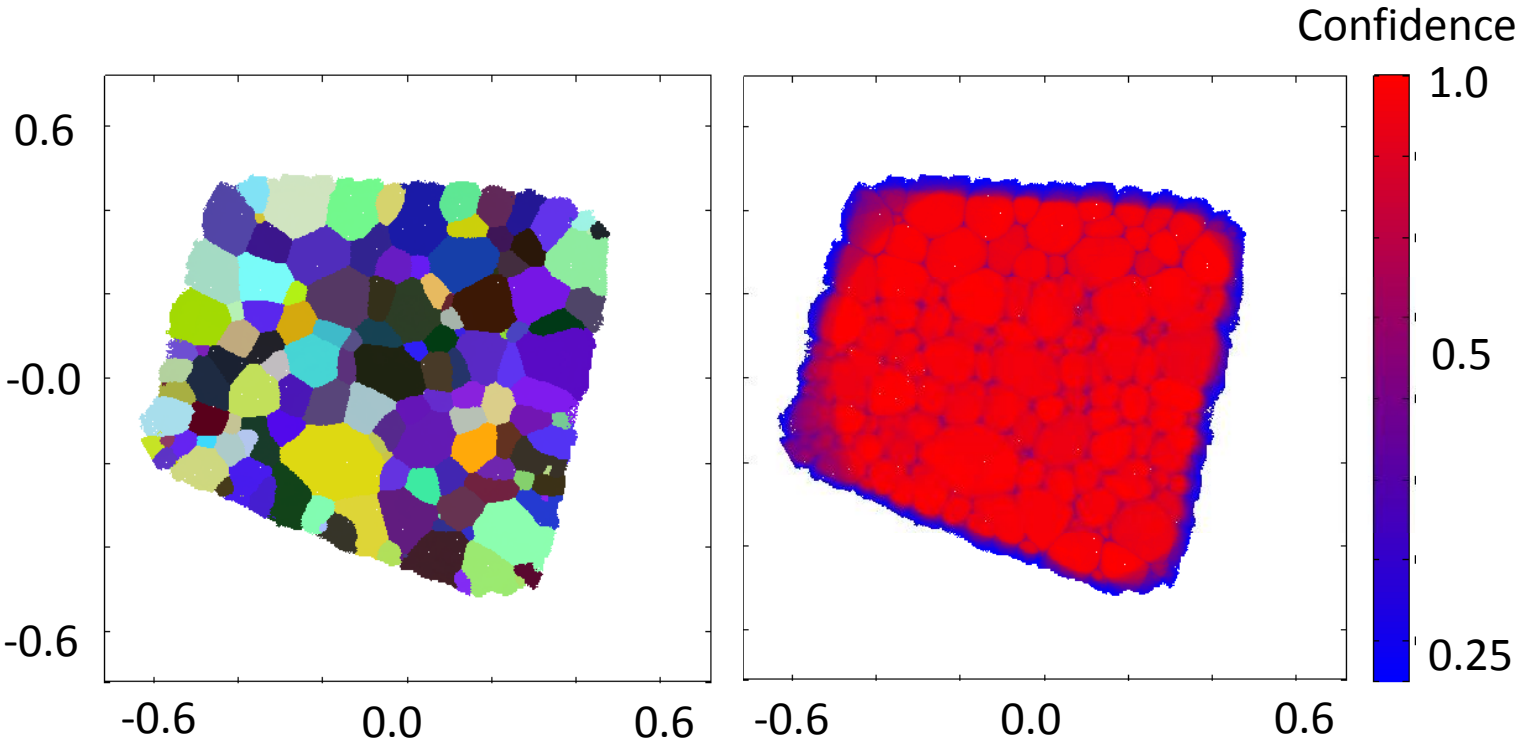

J. Lind

Annealed Zr

HEDM Microscope

Work flow

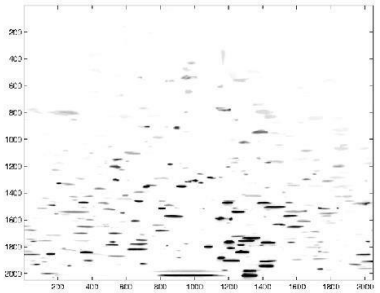

Diffraction Image
Collection
[12 - 18 hours/vol]
[8 MB/image]

⇒

GridFTP
to Orthos cluster
[real-time]
[~ 300 GB/vol]

⇒

Background subtraction
[15 min/layer, post-sweep]
[~ 60 GB/vol]

⇒

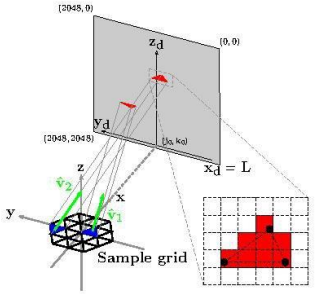

Monte Carlo
Parameter Optimization/
Test reconstructions
[2 - 4 hours]

⇓

Reduced data to
~ 10^3 core HPC

⇓

N layer
Reconstructions
TACC Ranger
[~ 10 GB/vol output]

Raw Output
.mic Files
[~ 10^7 voxels]

HEDM Microscope

Work flow

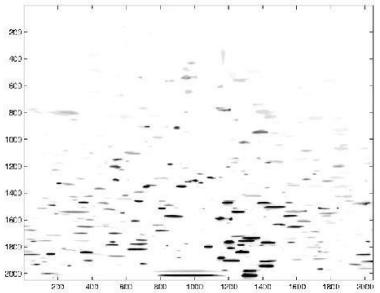

Diffraction Image
Collection
[12 - 18 hours/vol]
[8 MB/image]

⇒

GridFTP
to Orthos cluster
[real-time]
[∼ 300 GB/vol]

⇒

Background subtraction
[15 min/layer, post-sweep]
[∼ 60 GB/vol]

⇒

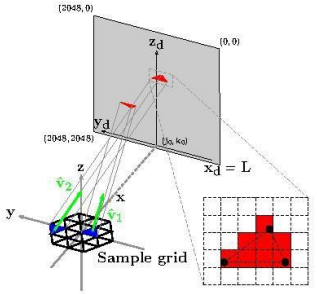

Monte Carlo
Parameter Optimization/
Test reconstructions
[2 - 4 hours]

⇓

Reduced data to
$\sim 10^3$ core HPC

⇓

N layer
Reconstructions
TACC Ranger
[∼ 10 GB/vol output]

←

Raw Output
.mic Files
[$\sim 10^7$ voxels]

←

2D Visualization

RF, Confidence Maps
Boundary lines
IGM, KAM

2D/3D Statistics

< Grain orientation >
IGM, KAM
Pole figures

3D Tet-Mesh Analysis

CGAL Library
Grain size, extraction, etc
GBCD

HEDM Microscope

Work flow

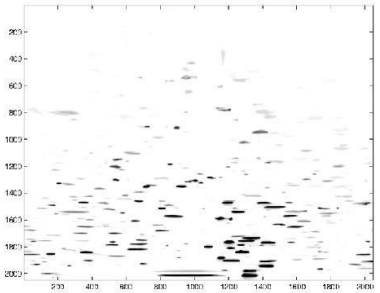

Diffraction Image
Collection
[12 - 18 hours/vol]
[8 MB/image]

$\Rightarrow$

GridFTP
to Orthos cluster
[real-time]
[$\sim$ 300 GB/vol]

$\Rightarrow$

Background subtraction
[15 min/layer, post-sweep]
[$\sim$ 60 GB/vol]

$\Rightarrow$

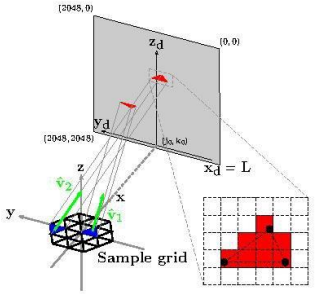

Monte Carlo
Parameter Optimization/
Test reconstructions
[2 - 4 hours]

$\Downarrow$

Reduced data to
$\sim 10^3$ core HPC

$\Downarrow$

N layer
Reconstructions
TACC Ranger
[$\sim$ 10 GB/vol output]

Raw Output
.mic Files
[$\sim 10^7$ voxels]

2D Visualization

RF, Confidence Maps
Boundary lines
IGM, KAM

2D/3D Statistics

< Grain orientation >
IGM, KAM
Pole figures

3D Tet-Mesh Analysis

CGAL Library
Grain size, extraction, etc
GBCD

Feature Tracking
Between States

Boundary motion
Twin evolution
Grain rotation
Sub-grain structure

What "Materials' Responses"?

- Mechanical: Elasticity
  - Reversible
  - Pretty well understood
  - Polymers
  - Crystals (anisotropic)

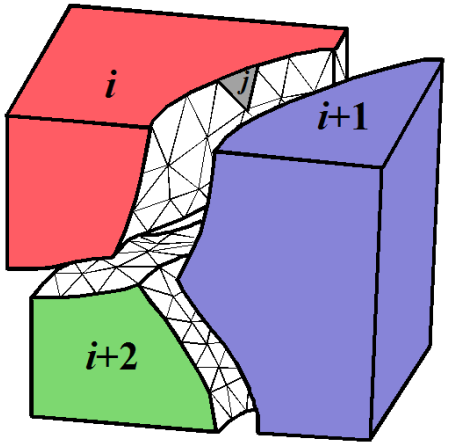

- Mechanical: Stretching a polycrystal – plastic response
  - Complex set of anisotropic constraints / interactions
  - Fatigue and failure
- Thermal: tending toward equilibrium / changing states
  - Surmounting energy barriers: cooking eggs
  - Melting ice / making steam
- Heating a polycrystal
  - Victory for the large and the orderly

Outline

1. nf-HEDM: data collection & orientation field reconstruction
   - Computational Forward Modeling Method
2. Example 1: Recrystallization in HP Aluminum
   - Reconstructions in heterogeneously damaged material
   - Recrystallization out of disordered regions
3. Example 2: Fatigue fracture surface in a Ni superalloy
   - Combined nf-HEDM & Tomography
   - Registration and interface region characterization
4. Combined near-field and far-field measurements
   - AFRL PUP: Ti-7Al orientation & strain tensor map
5. Summary and outlook

Intra-granular structure: pulled HP Al wire
What's resolvable?

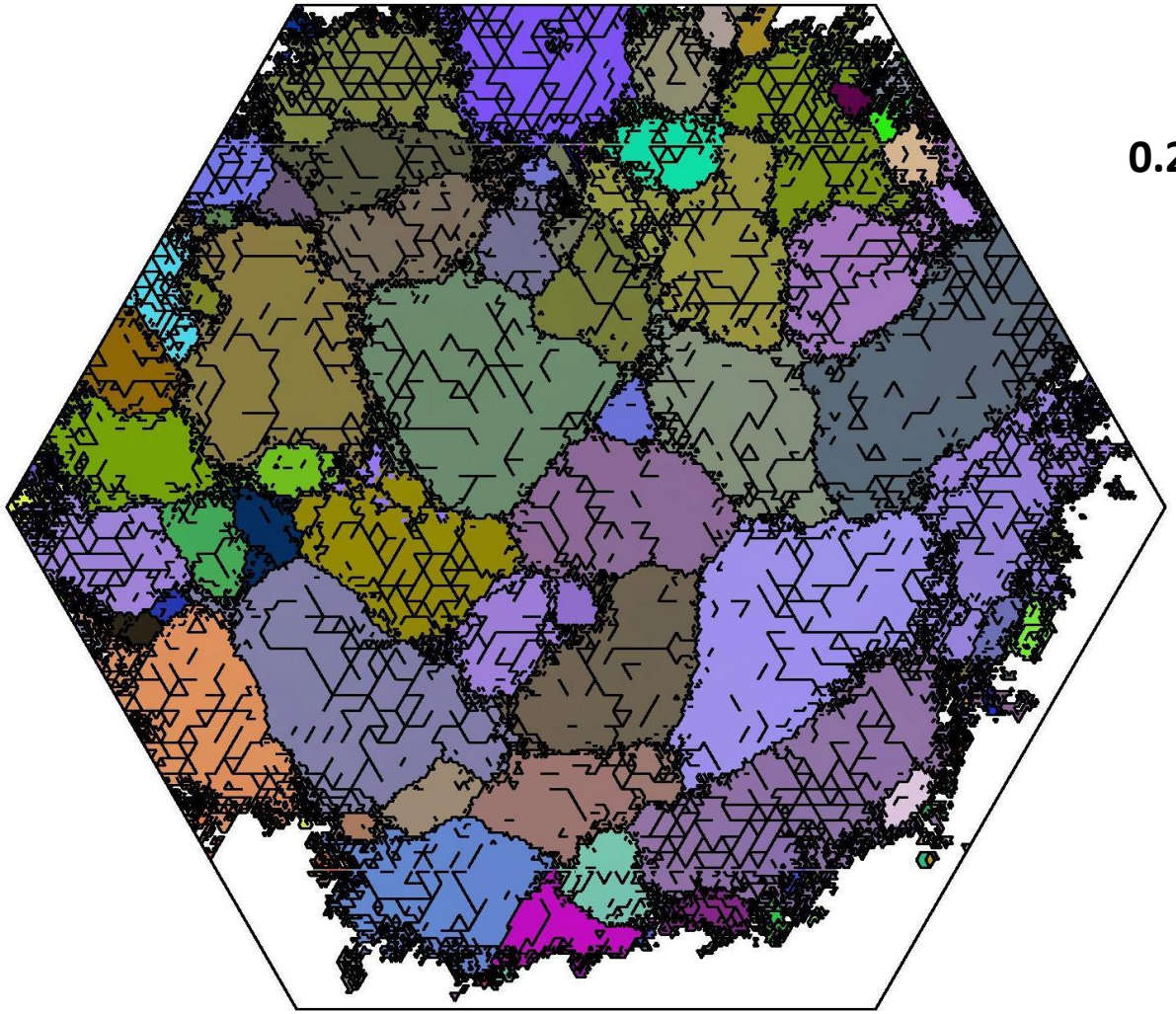

Hefferan et al, Acta Mat 2012

Recrystallization in pure Al

annealing

Voxel-based reconstruction shows new grain and nature of prior neighborhood

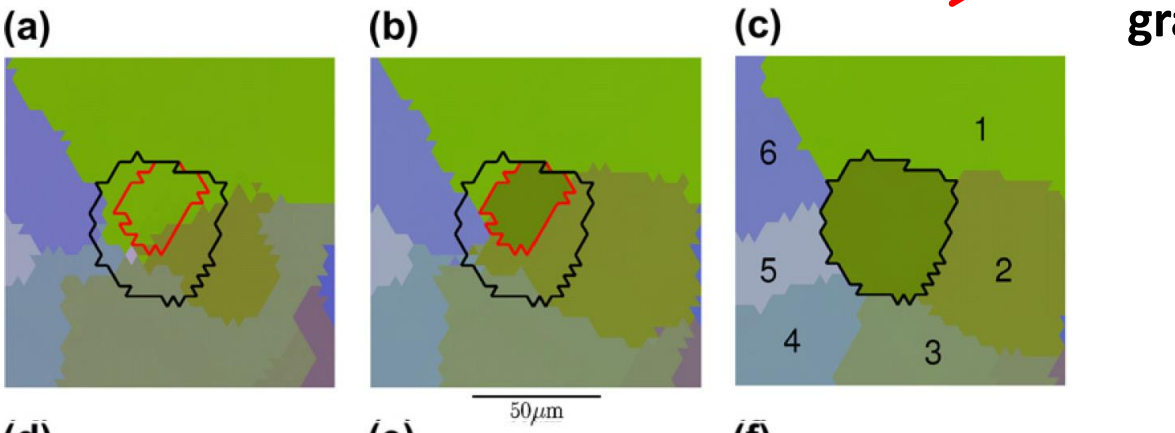

Lattice orientations

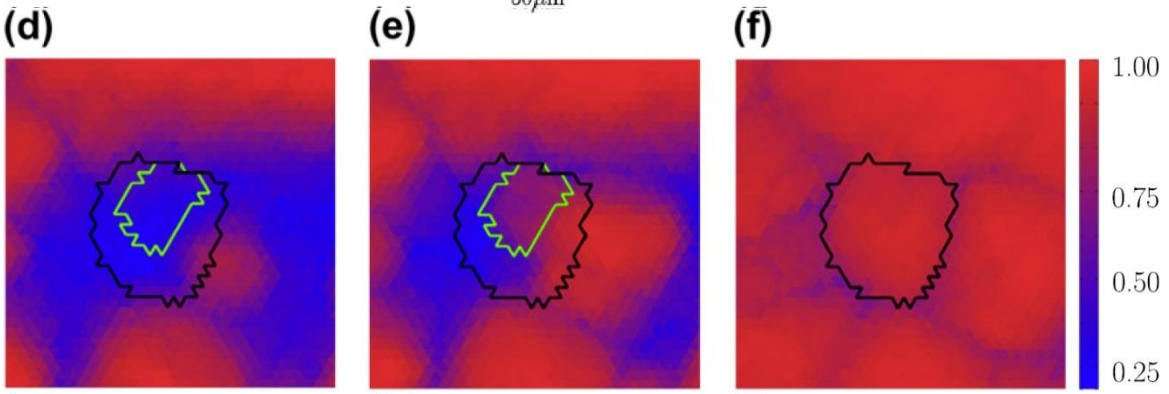

Confidence metric

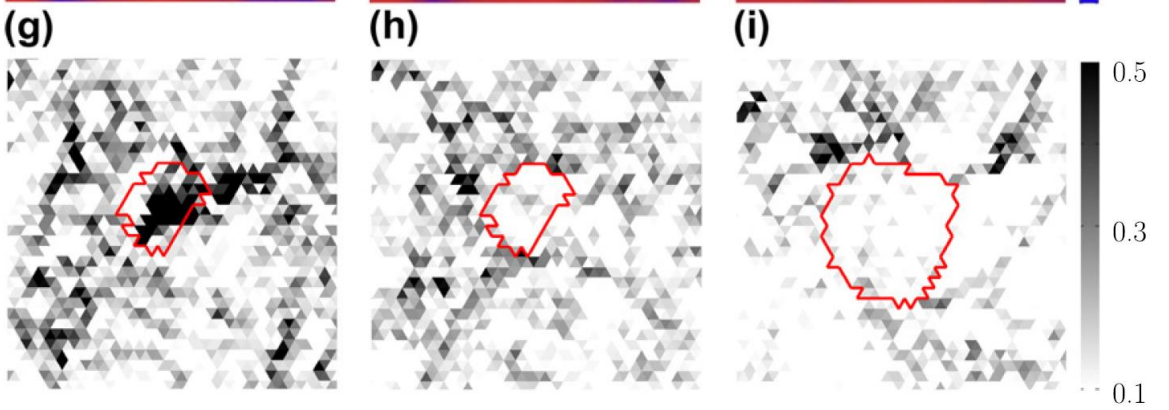

KAM map: 0.5 deg scale

Outline

1. nf-HEDM: data collection & orientation field reconstruction
   - Computational Forward Modeling Method
2. Example 1: Recrystallization in HP Aluminum
   - Reconstructions in heterogeneously damaged material
   - Recrystallization out of disordered regions
3. **Example 2: Fatigue fracture surface in a Ni superalloy**
   - **Combined nf-HEDM & Tomography**
   - **Registration and interface region characterization**
4. Combined near-field and far-field measurements
   - Ti-7Al: orientation & strain tensor map
5. Summary and outlook

Fatigue and Fracture in a Nickel Superalloy

- A strong, hard metallic alloy used in high temperature, high stress and corrosive environments
  - Aircraft and power generation turbines
  - Drill bits in wells
- Critical questions:
  - Where do cracks nucleate?
  - What determines the path of the fracture surface?
  - What are structural components required for reliable modeling?
- Microstructural characteristics
  - Crystal orientations relative to load
  - Grain boundary orientations relative to load
  - Grain boundary type distribution

Fatigue and Fracture in a Nickel Superalloy

- Questions for HEDM measurements
  - Can fatigued / deformed microstructures be mapped?
  - Registration of distinct modalities?

- Good news:
  - Tomo & HEDM can be done with same detector & setup
  - No sample handling

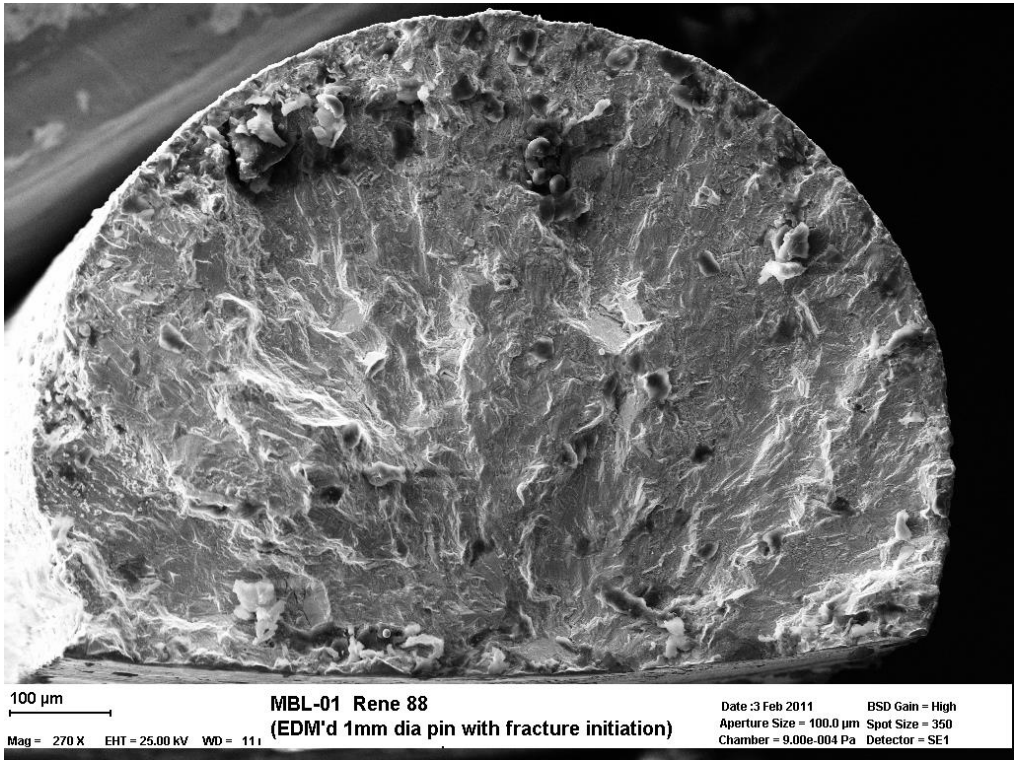

Experiment Schematic

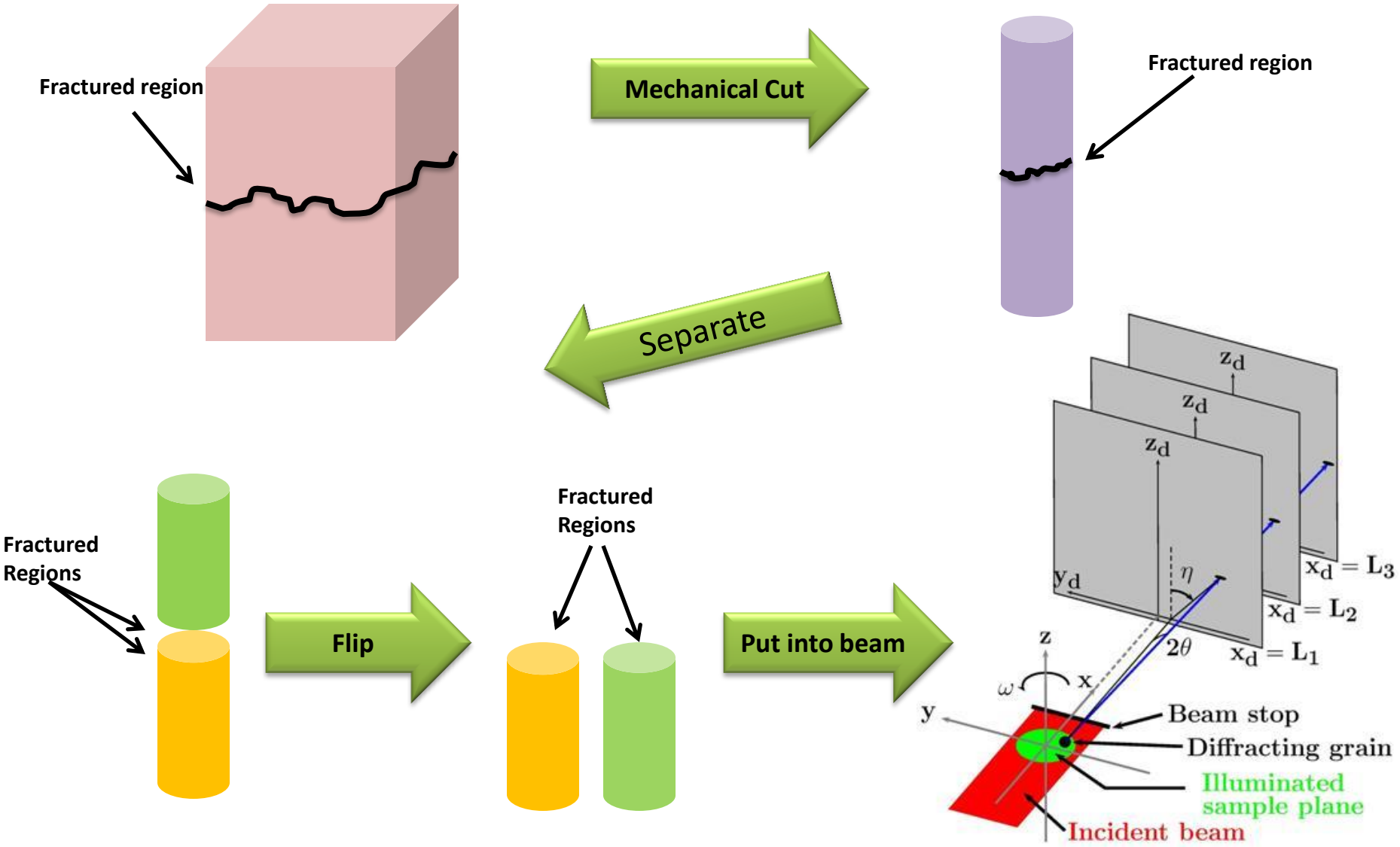

Fracture Surfaces: High Energy X-ray Tomography

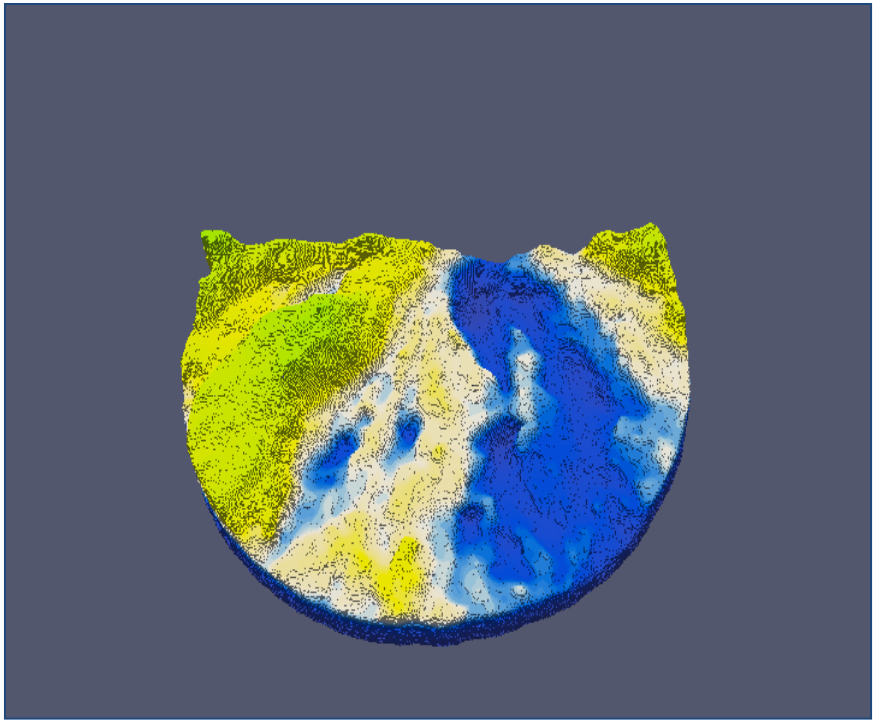

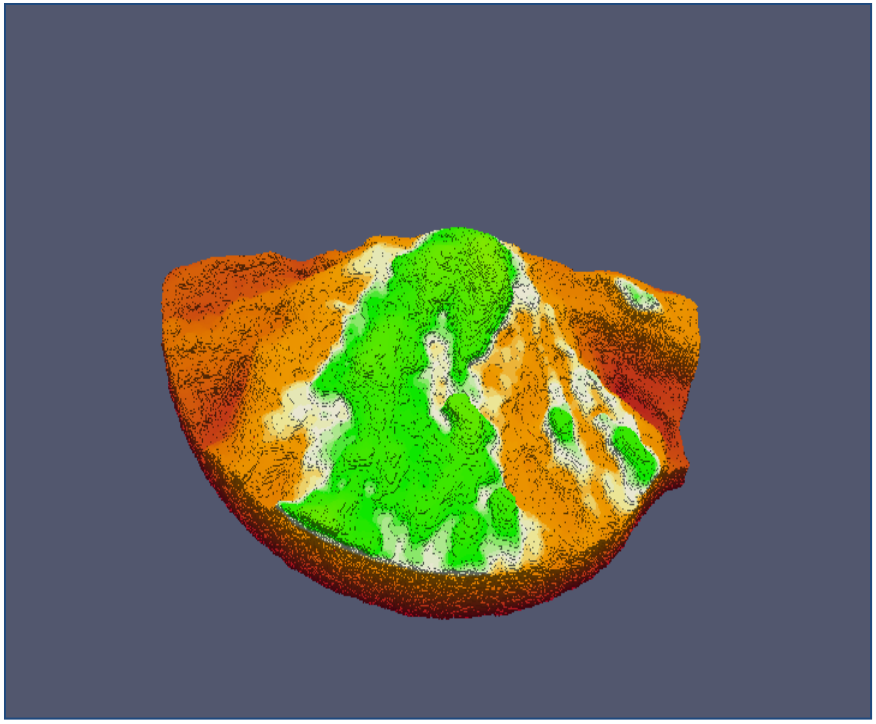

First Piece

Colored by height
Low = Blue
High = Green

Second Piece

Colored by height
Low = Red
High = Green

Detector Image: Single Crystal Grains

- One of 180 in 180 deg
- One of 360 per layer
- One of ~ 36,000 per volume
- 288 GB per volume
- ~3.6M diffraction spots

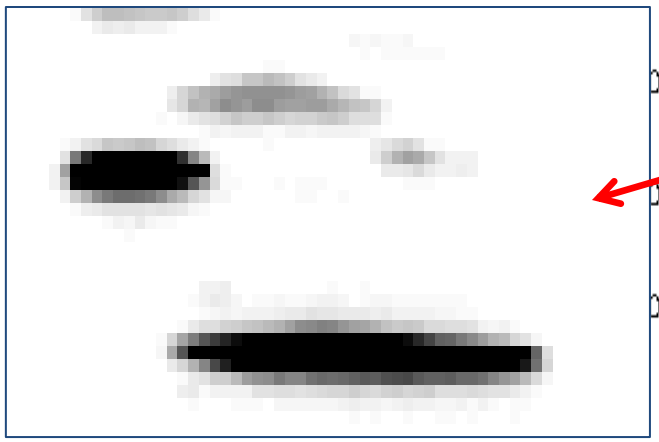

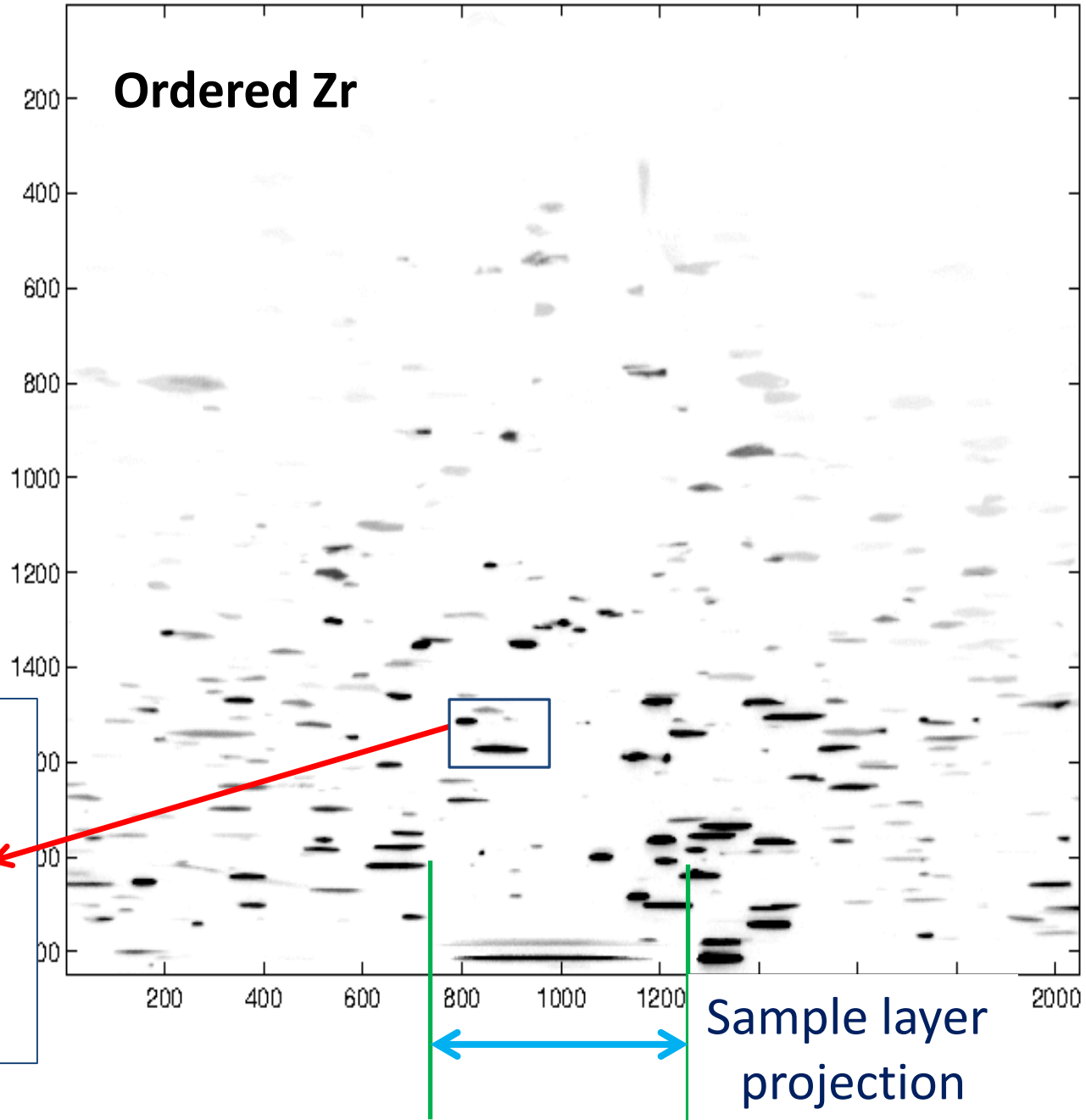

Fatigued/Fractured Superalloy Diffraction Image

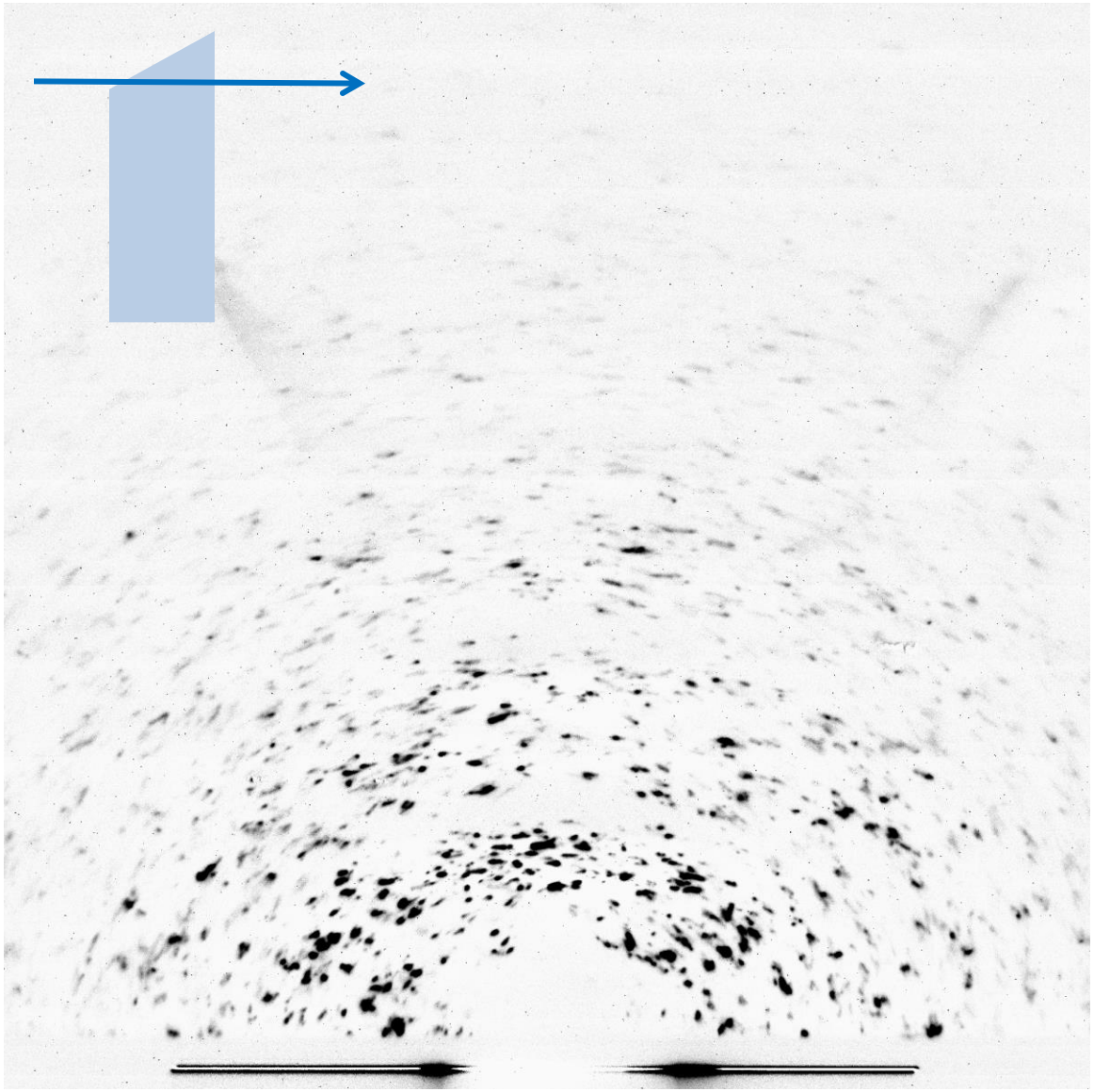

Layer 40 (z = 0.048 um)
As collected
diffraction image

Deep in bulk:

- **Full cross-section contributes**
- **Least damaged layer**

Arc-like patterns:
orientation gradients within grains -- scattering is broad in (η, ω)

Dense spot pattern:
Large number of small grains

Orientation and Confidence Maps: Two pieces reconstructed and rejoined

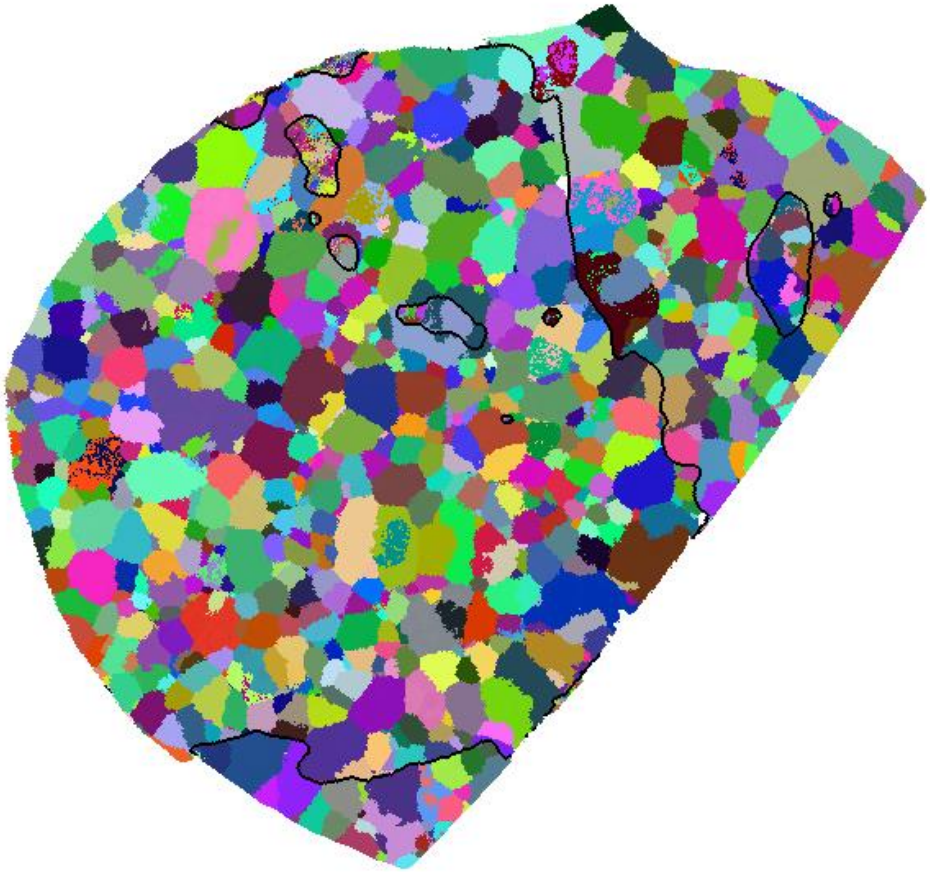

Orientations

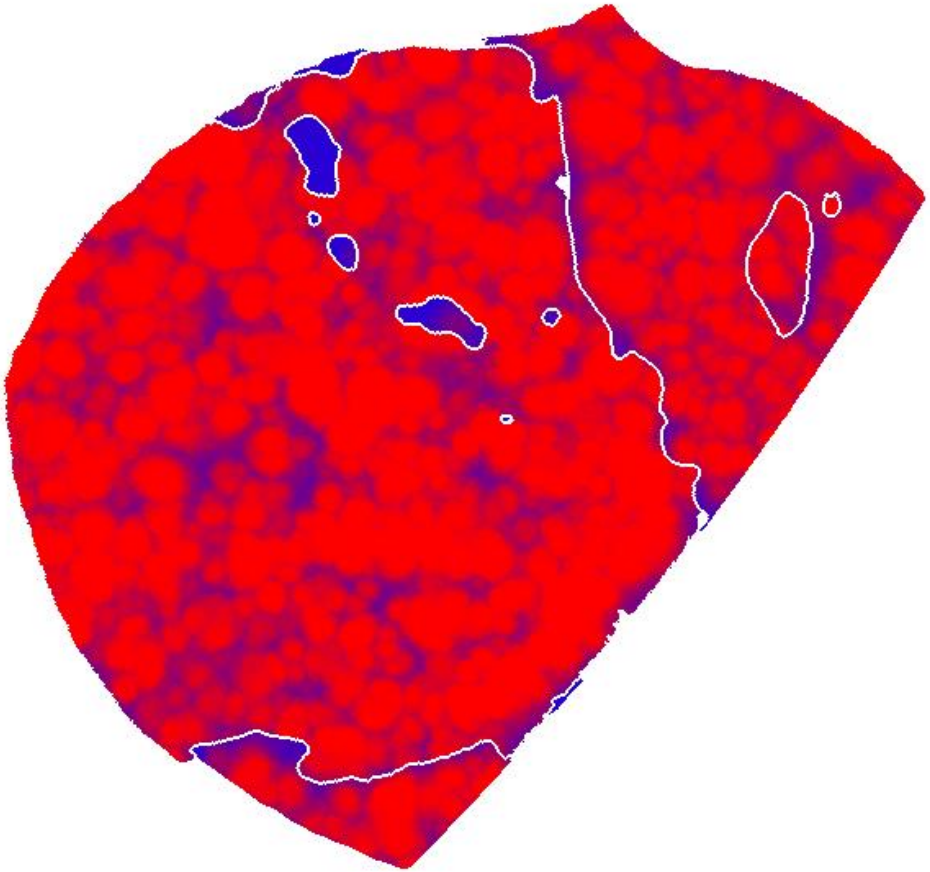

Confidence

Substantial Intra-granular Orientation Variation

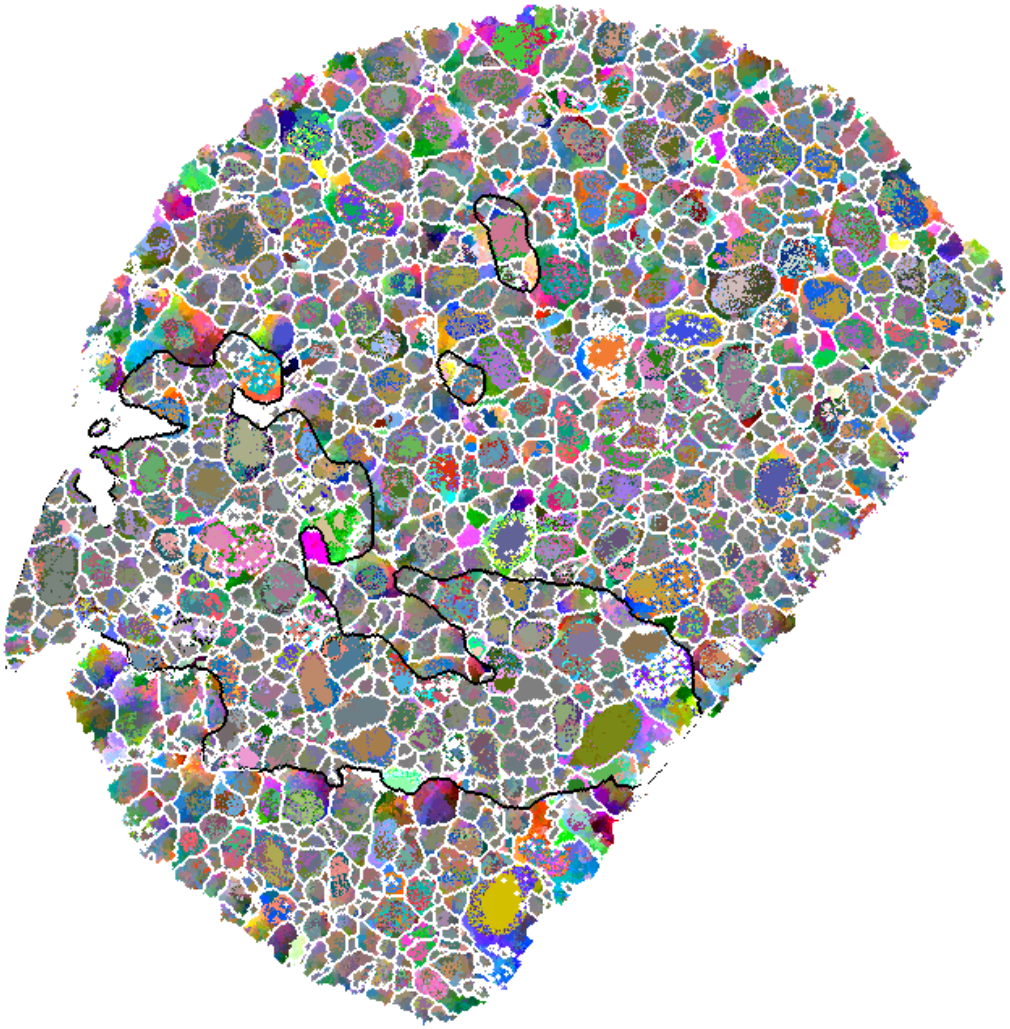

- White lines: boundaries with > 2 degree orientation discontinuity
- Colors: misorientation between voxel and grain averaged orientation
- Black lines: fracture surface intersection

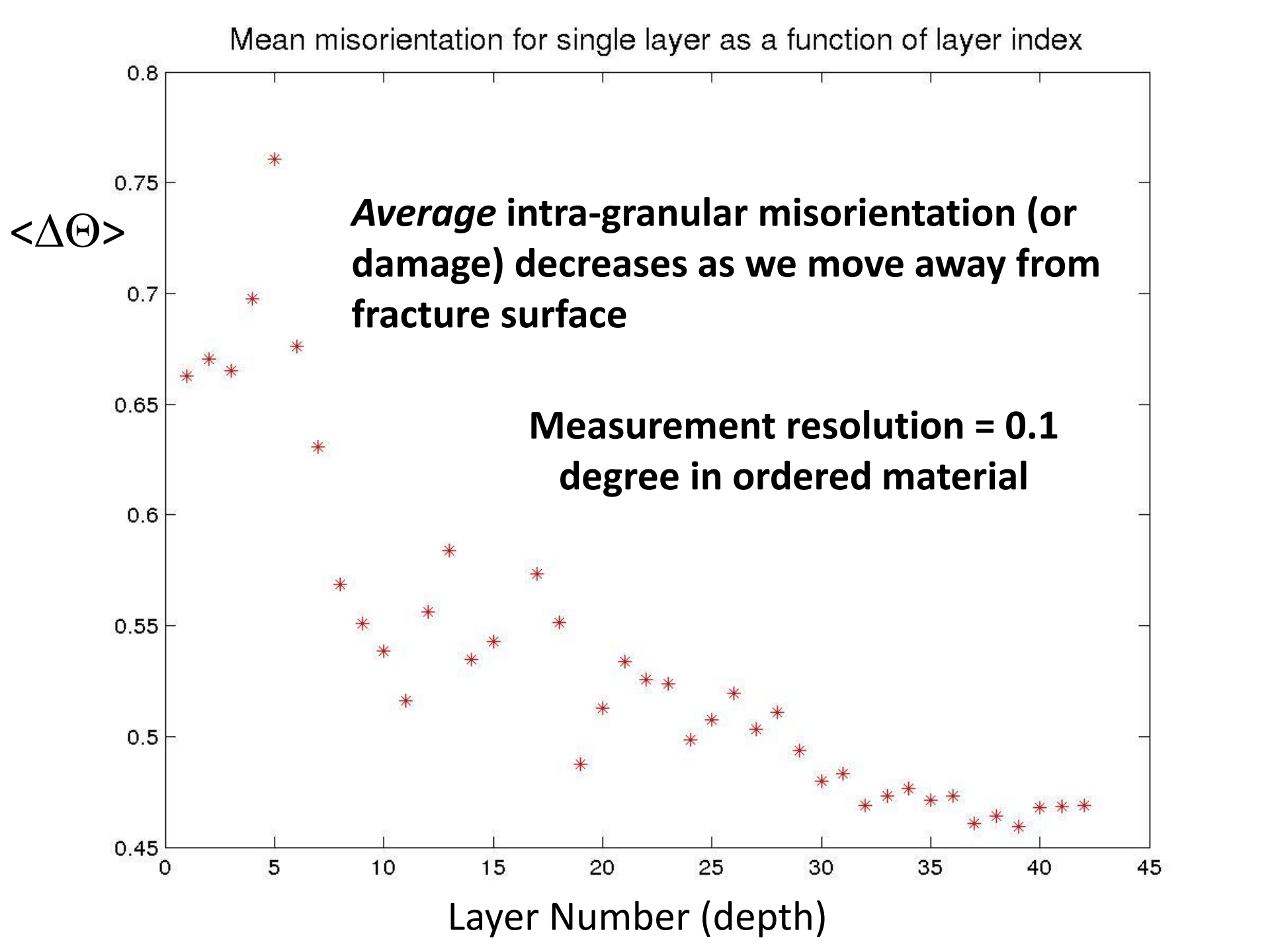
Mean misorientation for single layer as a function of layer index
<ΔΘ>
Average intra-granular misorientation (or damage) decreases as we move away from fracture surface
Measurement resolution = 0.1 degree in ordered material
Layer Number (depth)
0.8
0.75
0.7
0.65
0.6
0.55
0.5
0.45
0
5
10
15
20
25
30
35
40
45

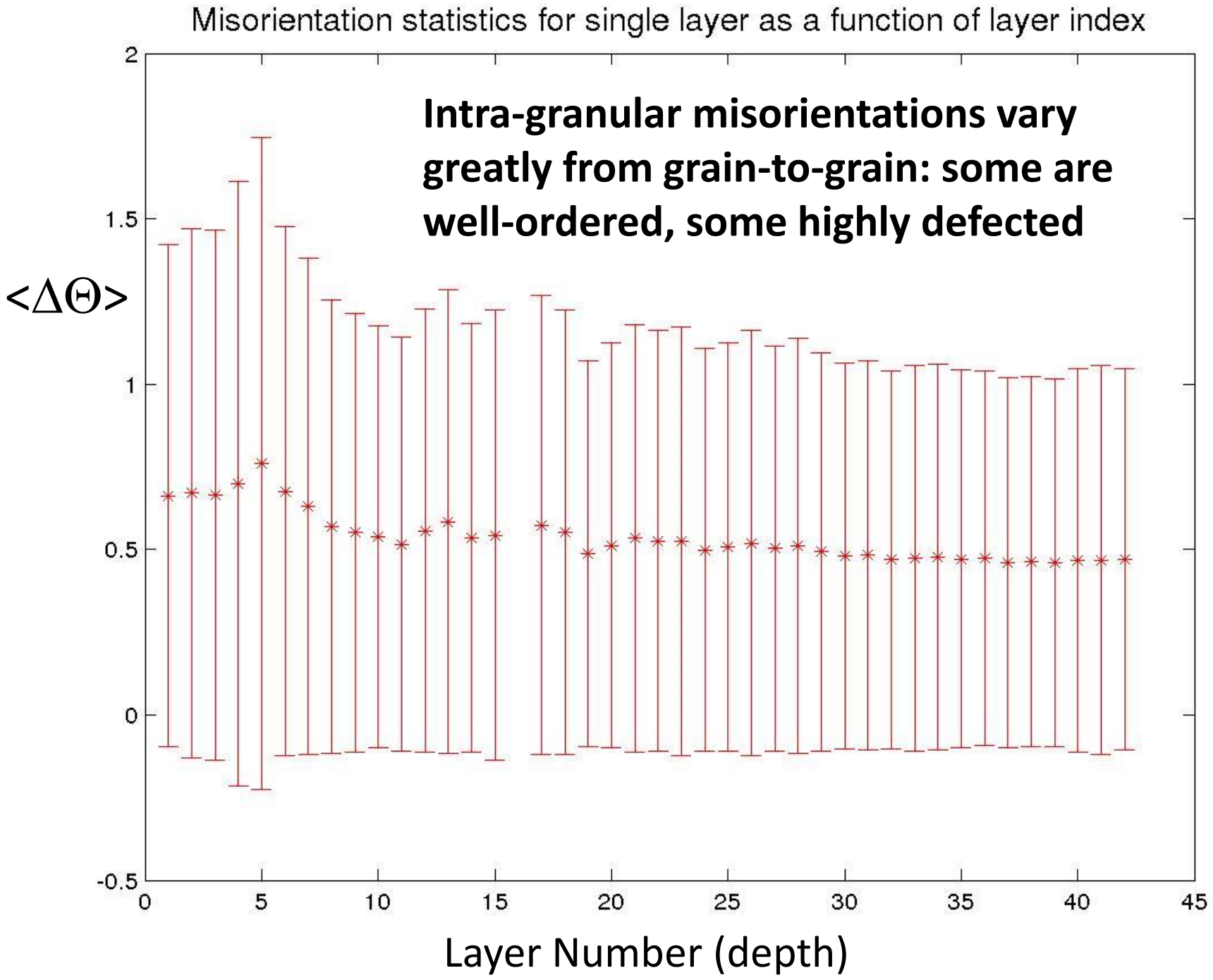
Misorientation statistics for single layer as a function of layer index
Intra-granular misorientations vary greatly from grain-to-grain: some are well-ordered, some highly defected
<ΔΘ>
Layer Number (depth)
2
1.5
1
0.5
0
-0.5
0
5
10
15
20
25
30
35
40
45

Alignment Procedures

First Piece Tomo

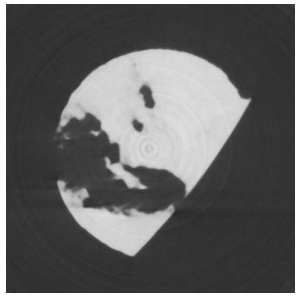

$T_t(x, y, z, \theta, \chi, \phi)$

Second Piece Tomo

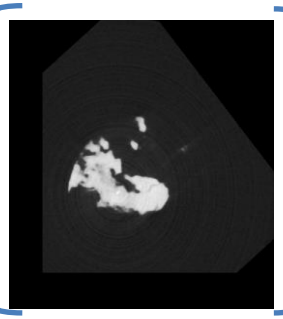

Combined Tomo

3D Aligned tomographic images

Density **L80** **Surface Contours**

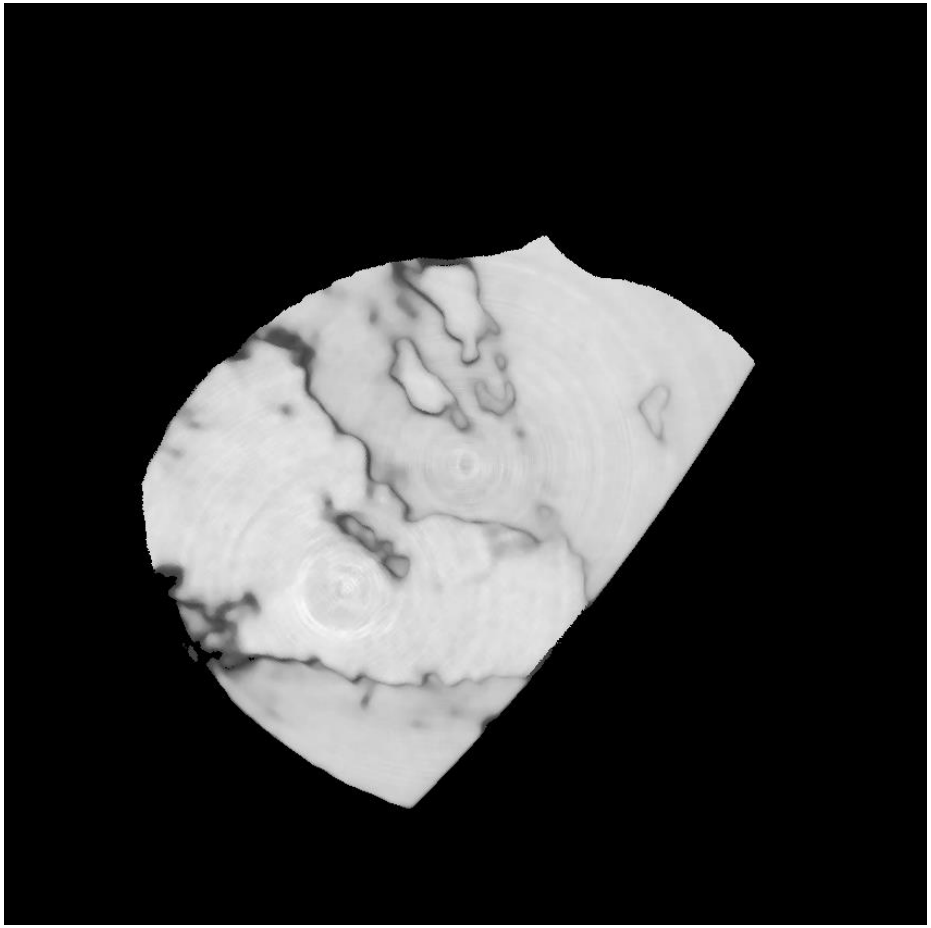

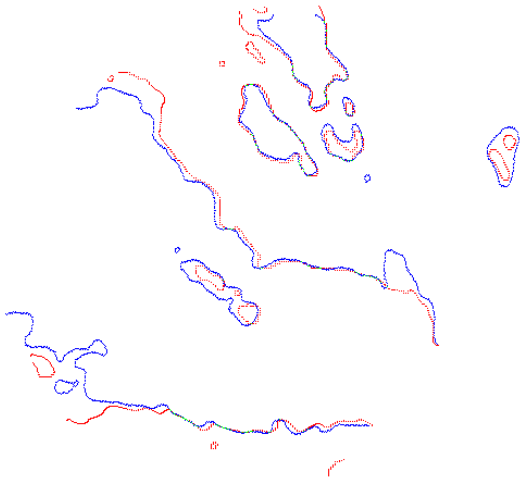

1 mm

3D Aligned tomographic images

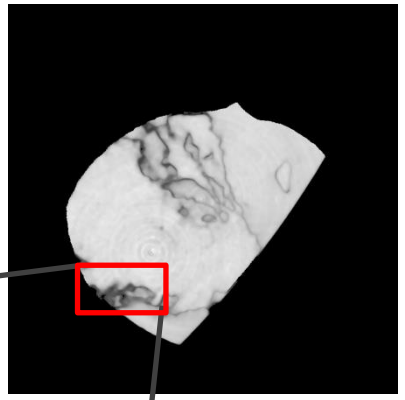

L75

Small amount of missing material

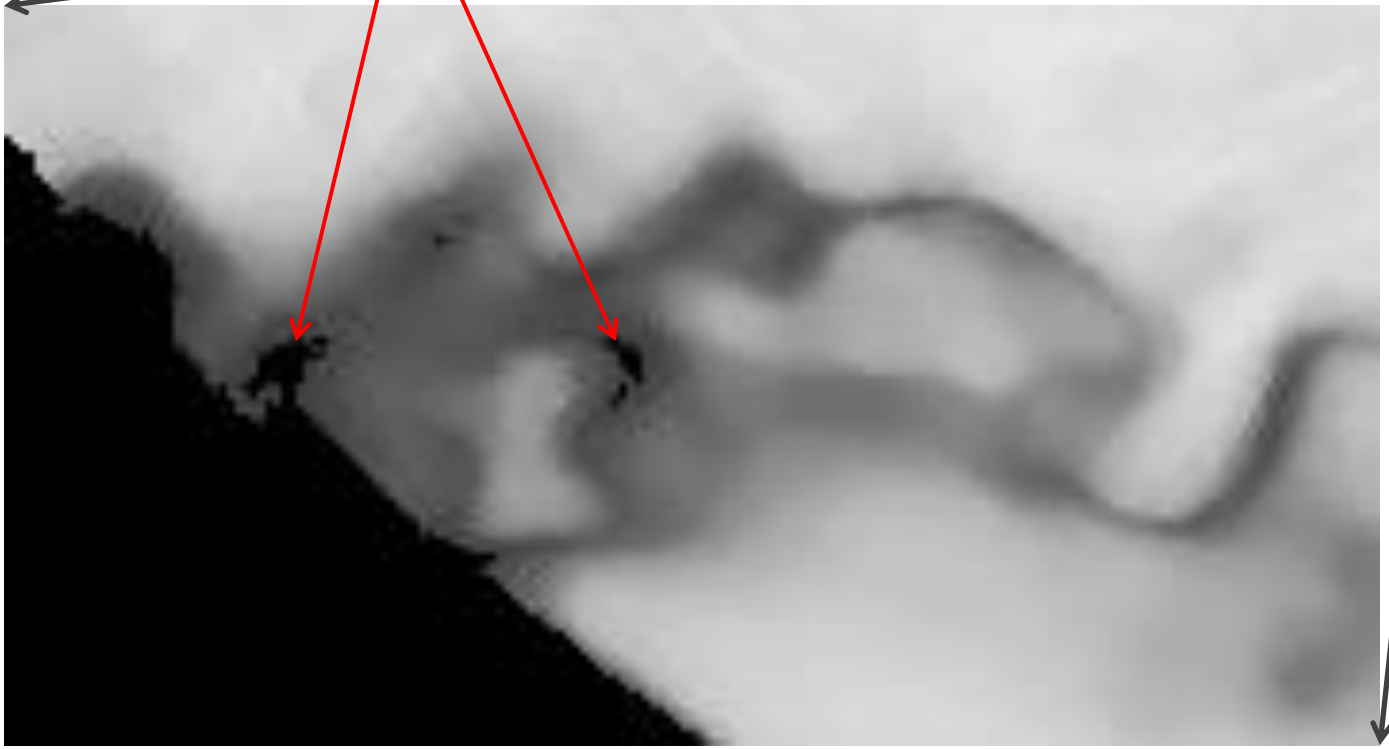

0.3 mm

Alignment Procedures

First Piece Tomo

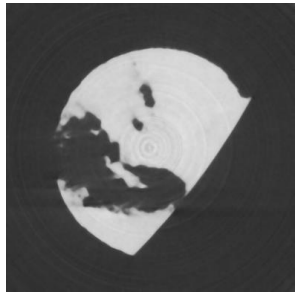

$T_t(x, y, z, \theta, \chi, \phi)$

Second Piece Tomo

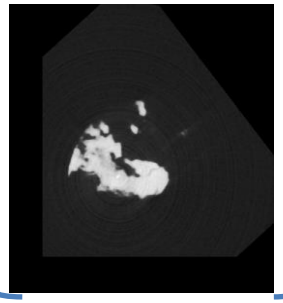

Combined Tomo

$Piece_i$ Tomo

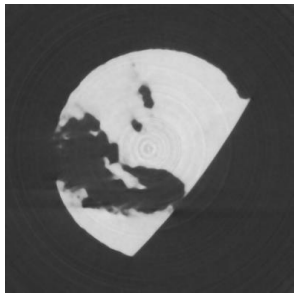

$T_{t\text{-}H}(z)$

$Piece_i$ HEDM

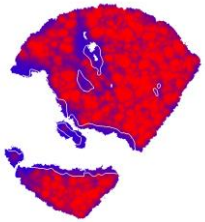

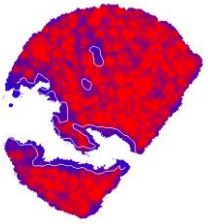

HEDM – Tomography Alignment

- Confidence metric estimates surface for each piece
- Optimize HEDM and Tomo surfaces
- z-translation constrained to less than HEDM layer spacing

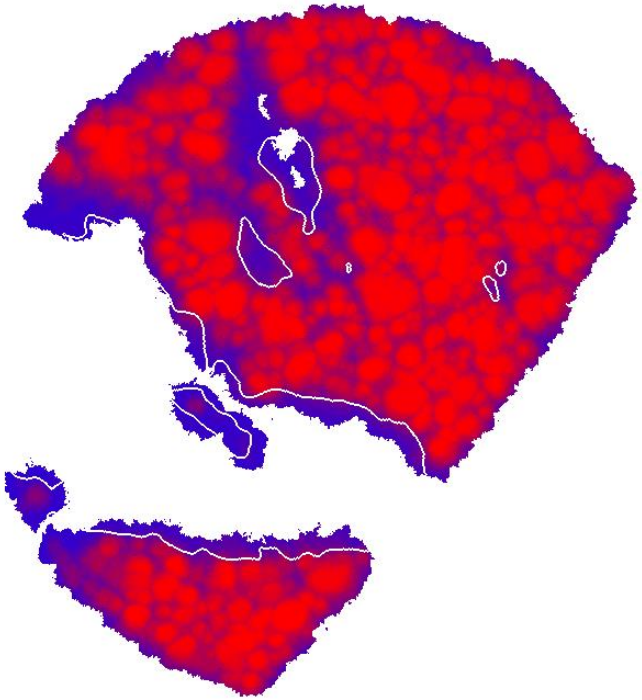

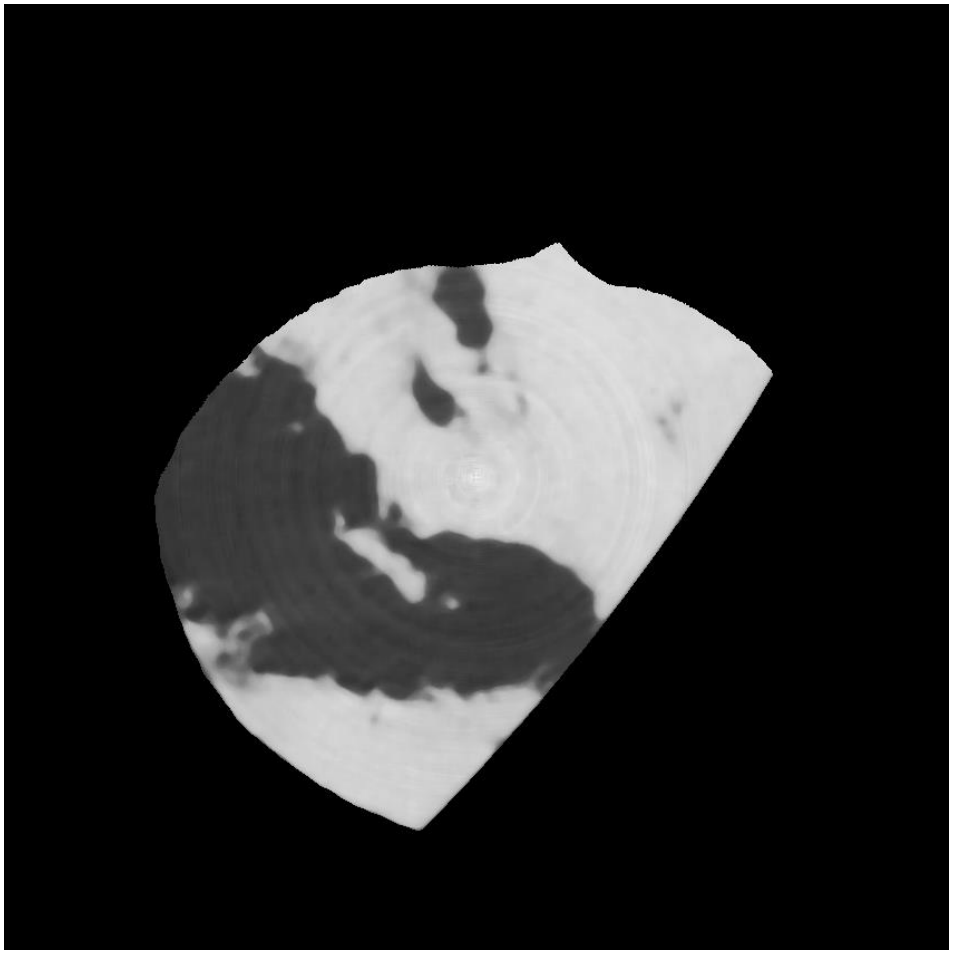

Alignment Procedures

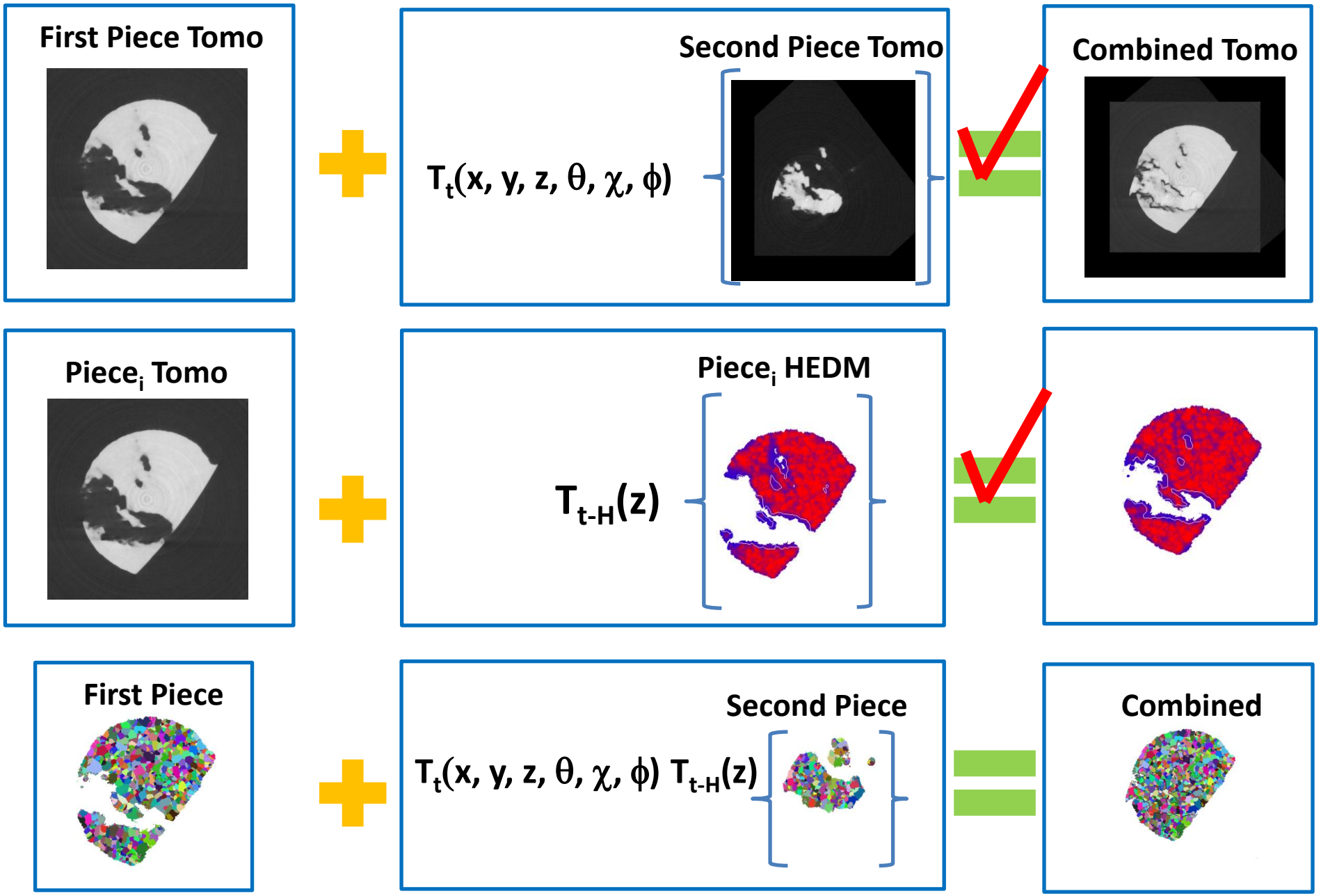

Merged Data: 3D Orientations, Fracture Surface, Uncertainty

L21_7

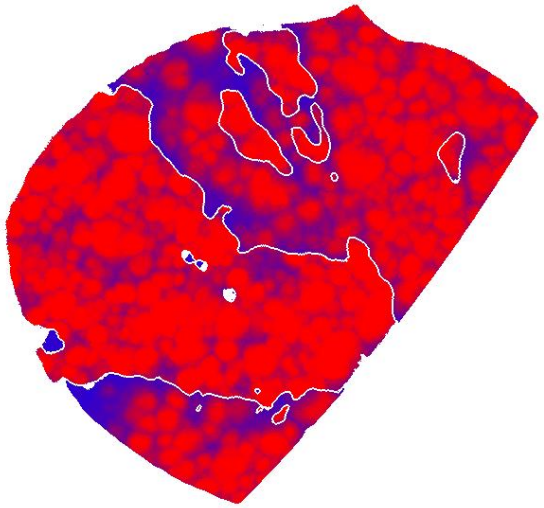

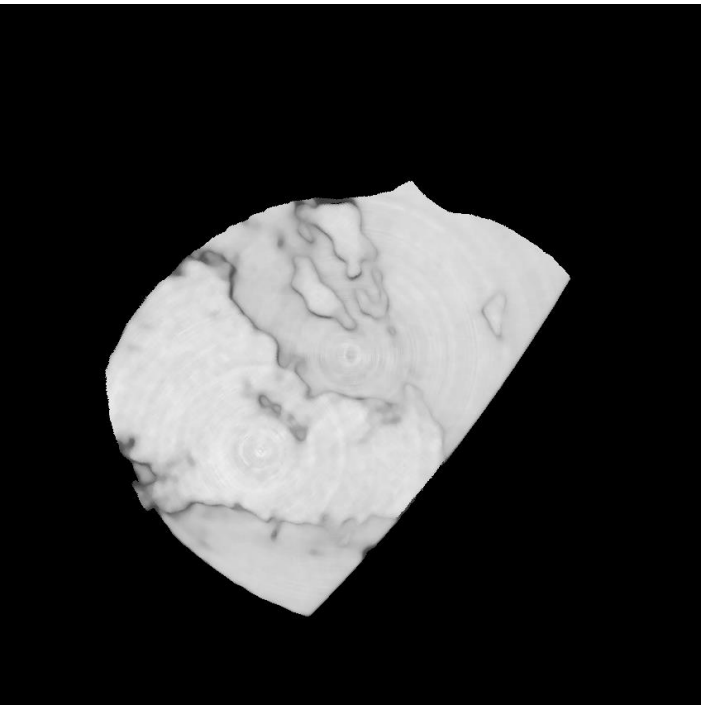

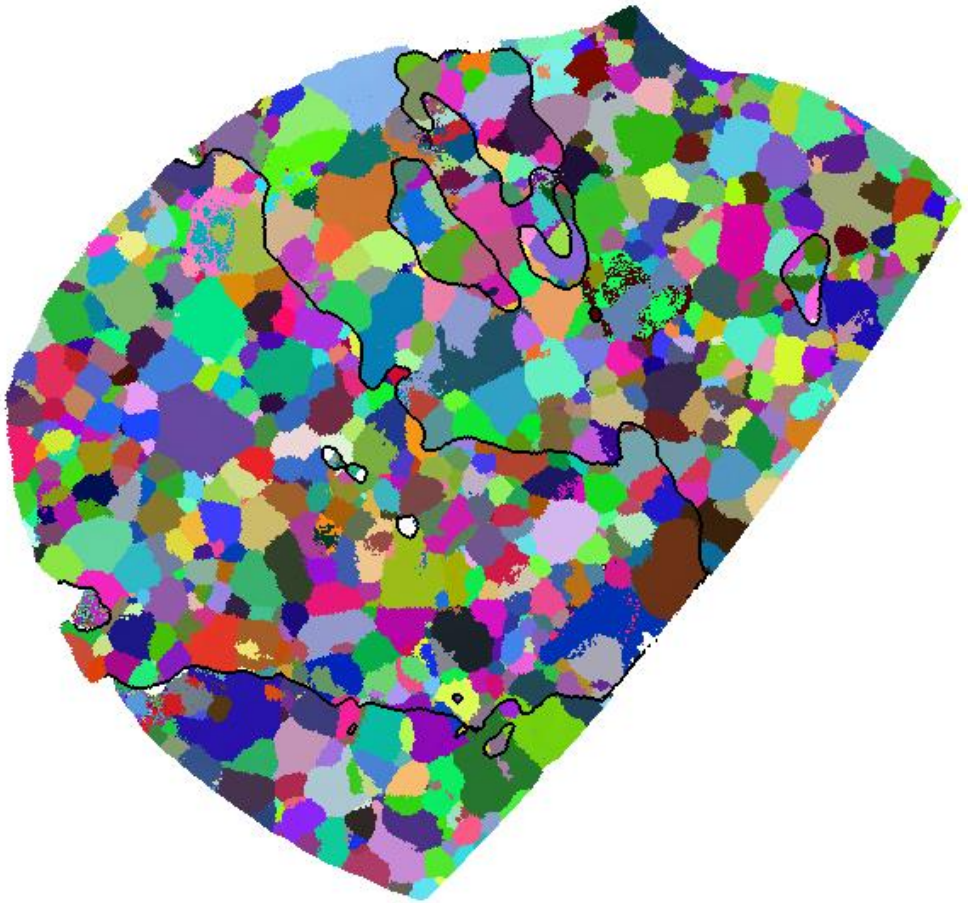

Alignment Procedures

First Piece Tomo

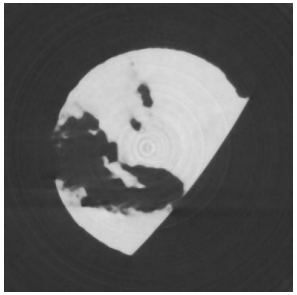

$T_t(x, y, z, \theta, \chi, \phi)$

Second Piece Tomo

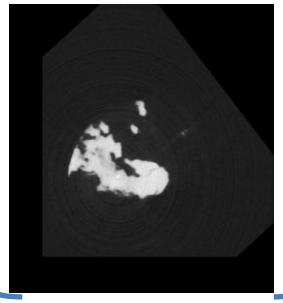

Combined Tomo

$Piece_i$ Tomo

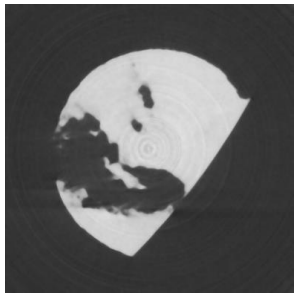

$T_{t\text{-}H}(z)$

$Piece_i$ HEDM

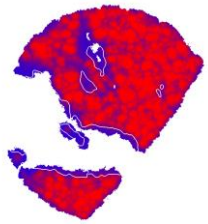

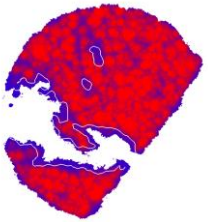

First Piece

$T_t(x, y, z, \theta, \chi, \phi)$ $T_{t\text{-}H}(z)$

Second Piece

Combined

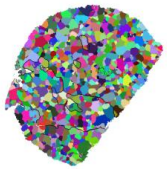

Observed Mesoscale Responses

Fatigue fracture in aerospace Ni superalloy

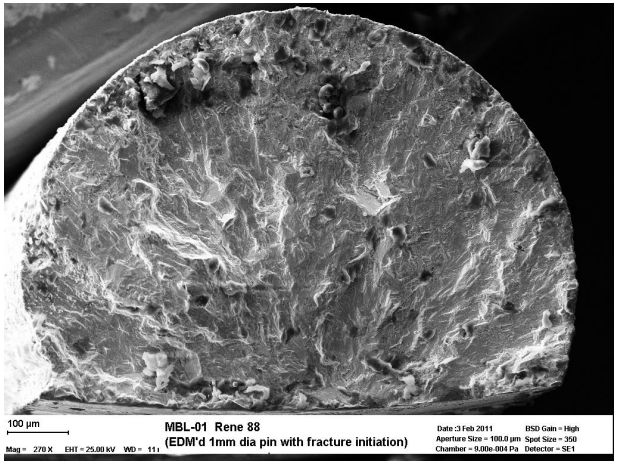

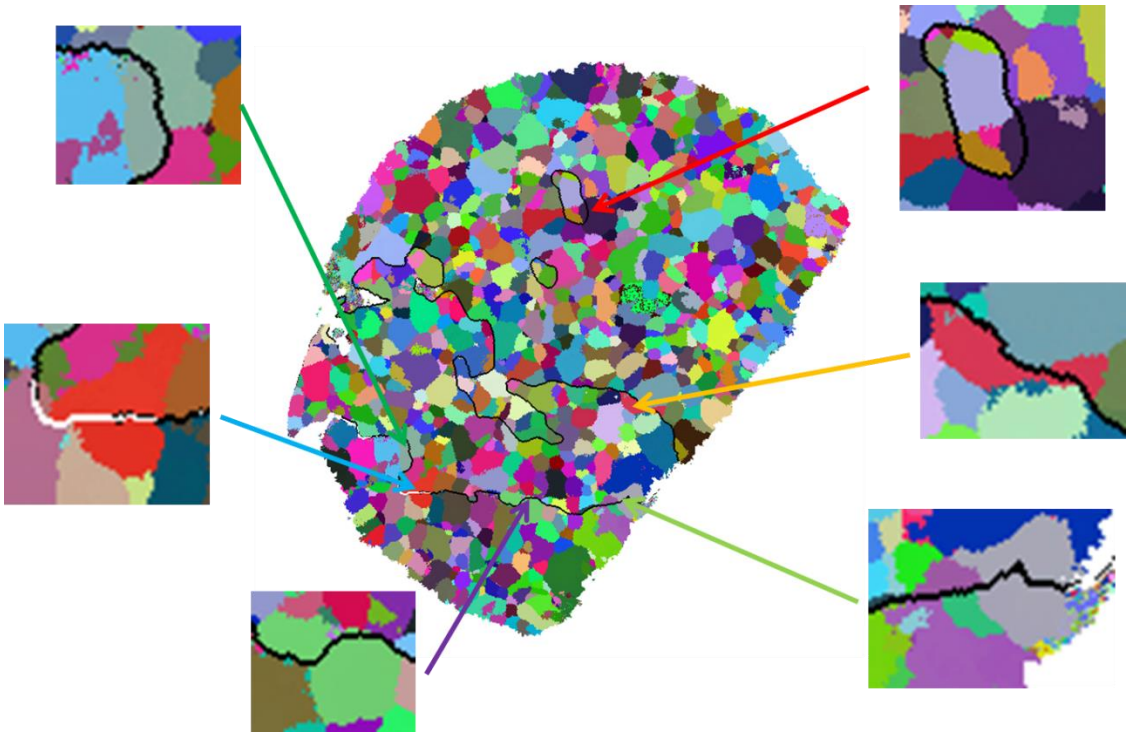

Tan, et al, in preparation

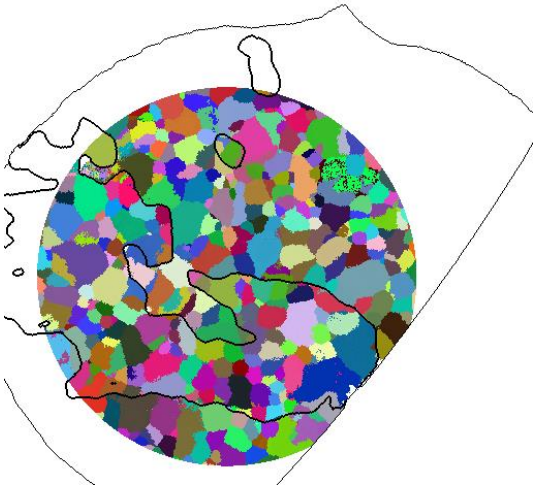

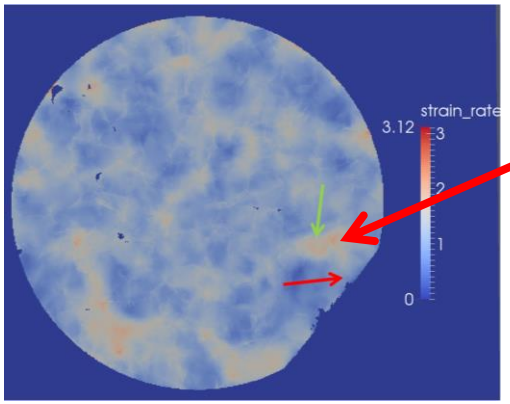

Computed stress hot spot near observed fracture initiation

Fracture Surface Statistics: Current Work

- Compute local surface normals from tomography
- Determine crystal axes along normals
- Determine inter-granular grain boundary fracture
- Determine intra-granular fracture orientation
- Comparison to plasticity model computations using orientation reconstruction as starting point
- Next: In-situ / pre-fracture evolution of microstructure with strain sensitivity added

Current Developments at APS Sector 1: Multi-modal Measurement and Analysis

- AFRL led Partner User Program (PUP) allocation
  - Technique/hardware development
    - Combined nf- and ff-HEDM and tomography and…
    - Tension/compression/cycling at elevated T
  - Analysis code development
  - Collaboration: AFRL, APS, LLNL, CMU, CHESS/Cornell
- APS Upgrade: 10 – 50 X brilliance, stability, new fixed E beam line

- Near-field HEDM: orientation mapping and tracking
- Far-field HEDM: grain/cross-section averaged strain tensors
- HE-tomography: sample shape, inclusions, cracks, void tracking

Currently at 1-ID taking data!

Far-field Measurement

- Position on detector: G_{hkl} in lab → G_{hkl} in sample frame
  - Crystallographically consistent $\{G_{hkl}\}$: orientation determination (fast)
  - Centers of mass of $\{G_{hkl}\}$'s: grain centers of mass
- Radial motions: strain sensitivity
  - $\{(\Delta d/d)_{hkl}\}$ → ε_{ij}

Mutual benefits of nf- & ff- combination

- ff into nf: accelerated orientation search
- nf into ff: complete knowledge of microstructural neighborhood along with strain state of grains

Combining nf- and ff-HEDM: AFRL-PUP
APS 1-IDE hutch

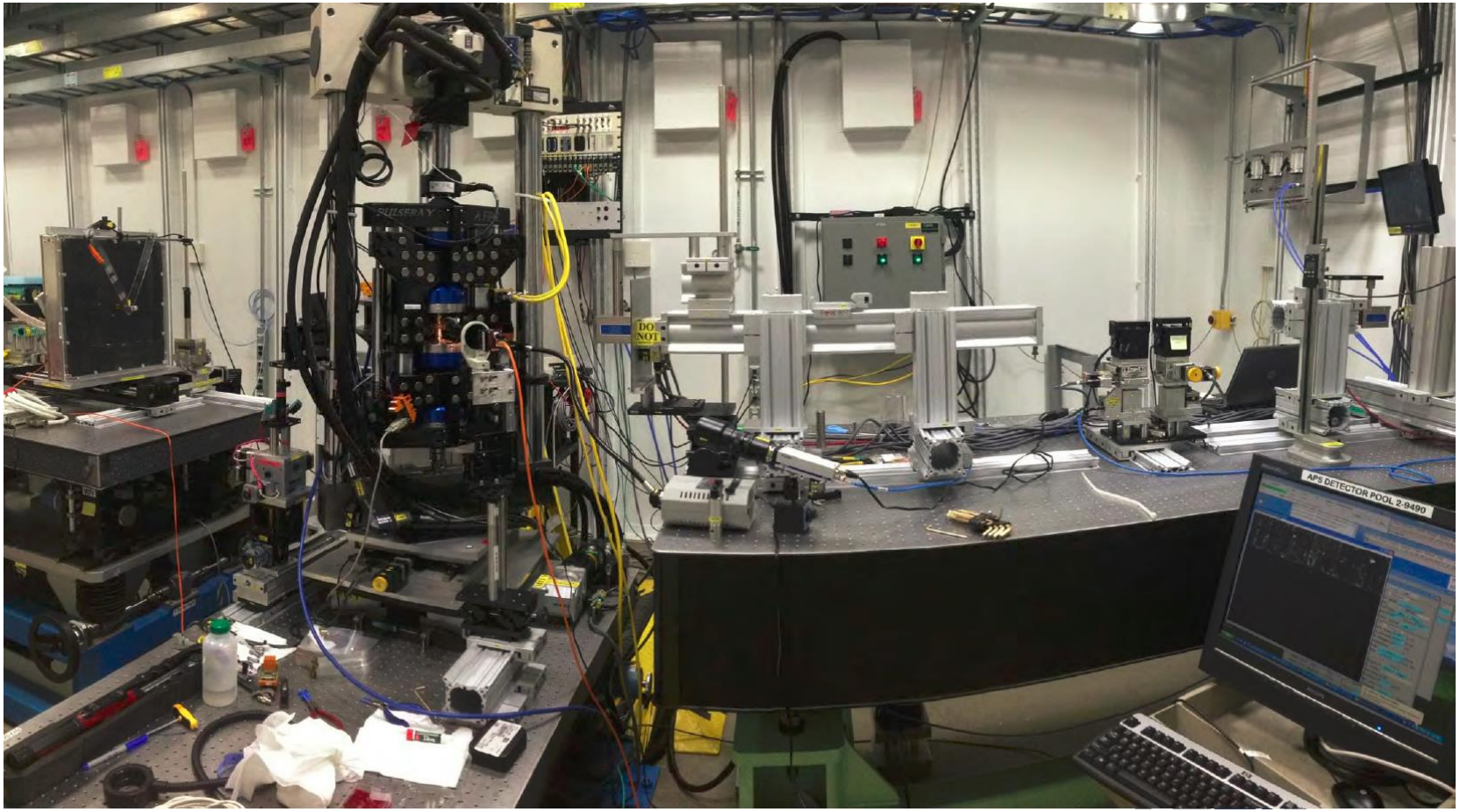

J. Schuren, P. Shade, T.J. Turner (AFRL)
J. Park, P. Kenesei, J. Almer, A. Mashayekhi, K. Goetze, E. Benda (APS)
S.F. Li, J. Lind, J. Bernier (LLNL), D. Menasche, R.M. Suter (CMU), B. Blank (PulseRay)

Combining nf- and ff-HEDM: AFRL-PUP
APS 1-IDE hutch

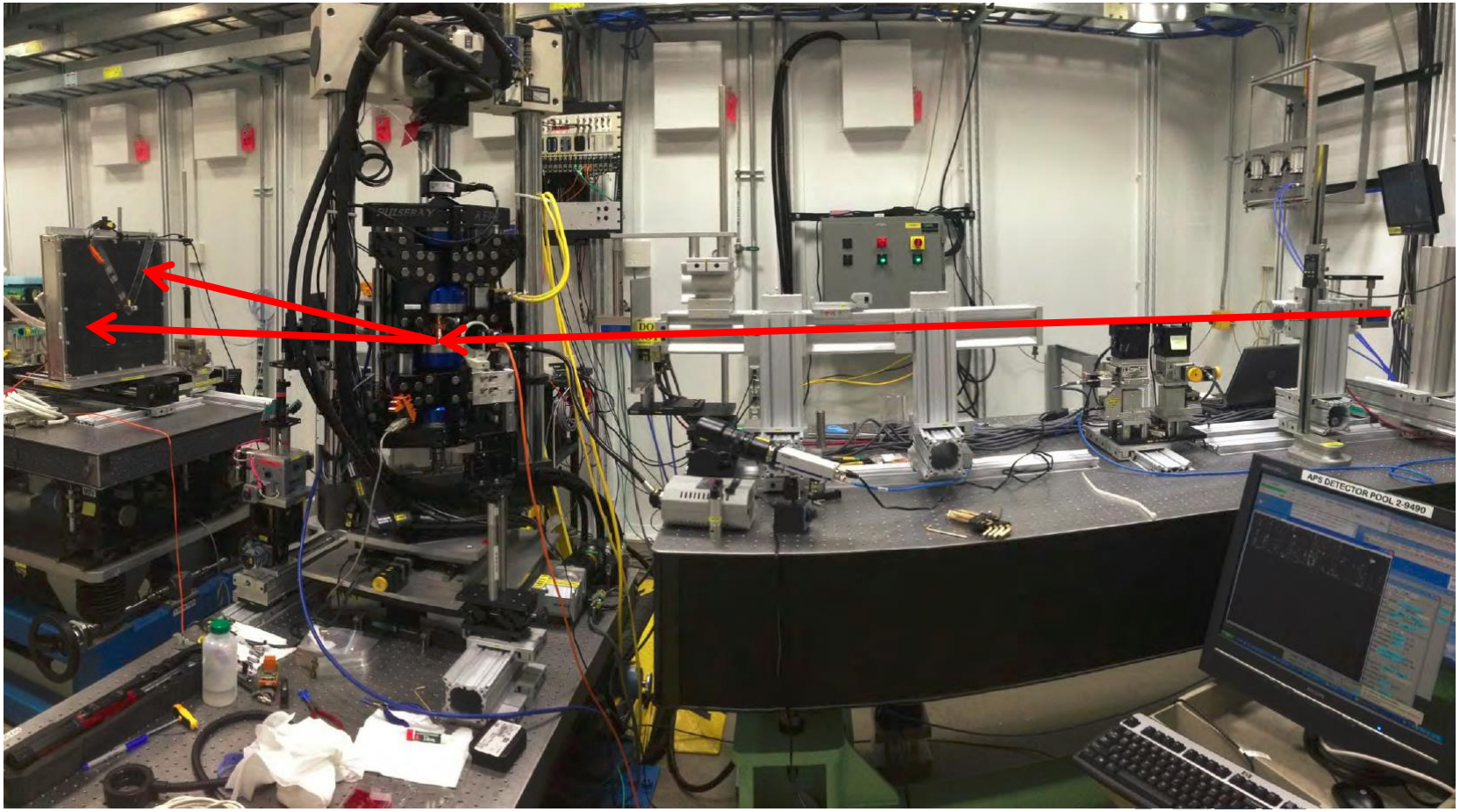

J. Schuren, P. Shade, T.J. Turner (AFRL)
J. Park, P. Kenesei, J. Almer, A. Mashayekhi, K. Goetze, E. Benda (APS)
S.F. Li, J. Lind, J. Bernier (LLNL), D. Menasche, R.M. Suter (CMU), B. Blank (PulseRay)

AFRL in-situ loading apparatus
Full rotation under load

Far Field Detector

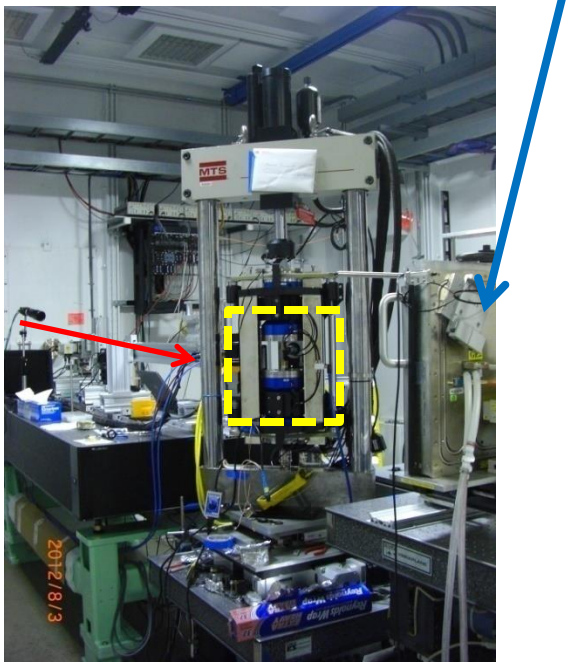

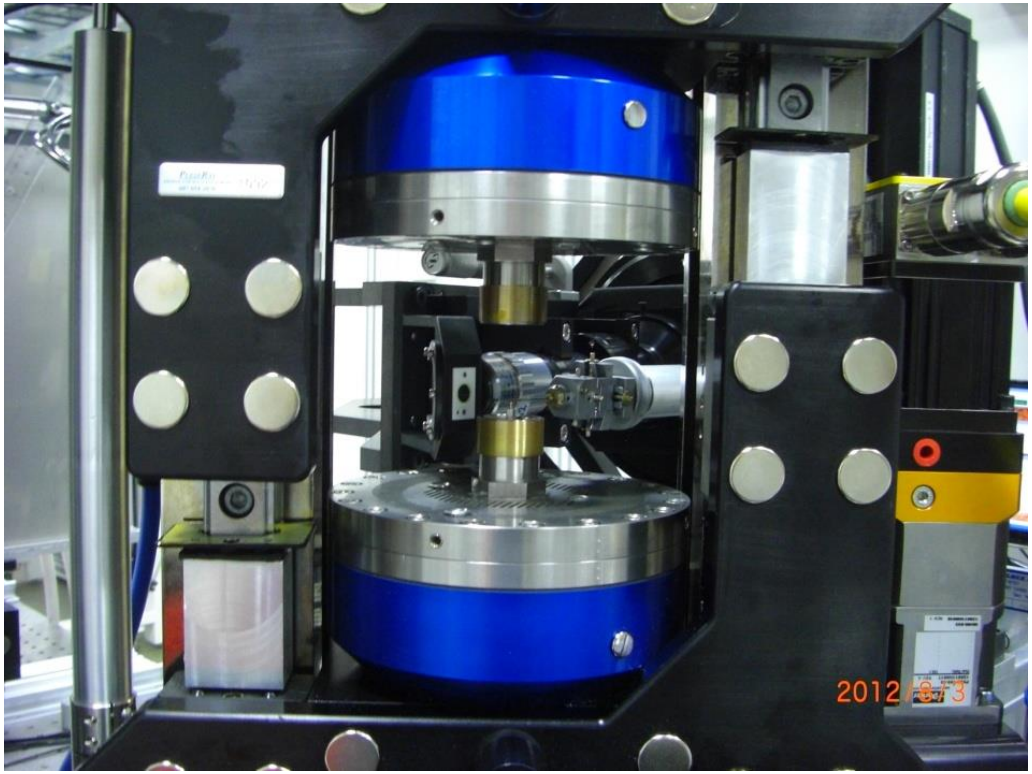

AFRL in-situ loading apparatus
Full rotation under load

Sample grips

Air bearings

Far Field Detector

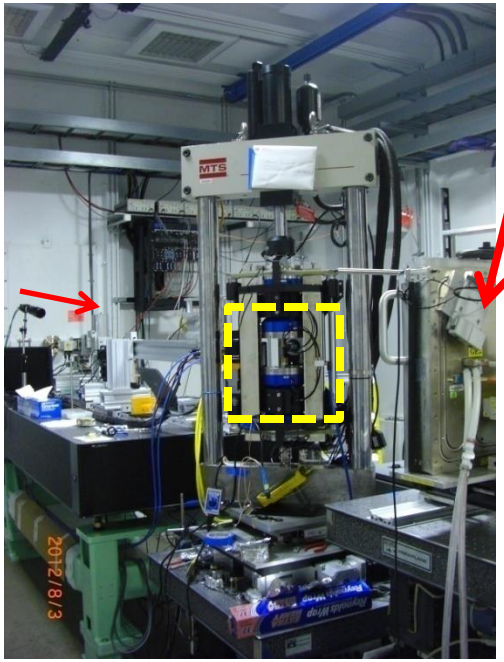

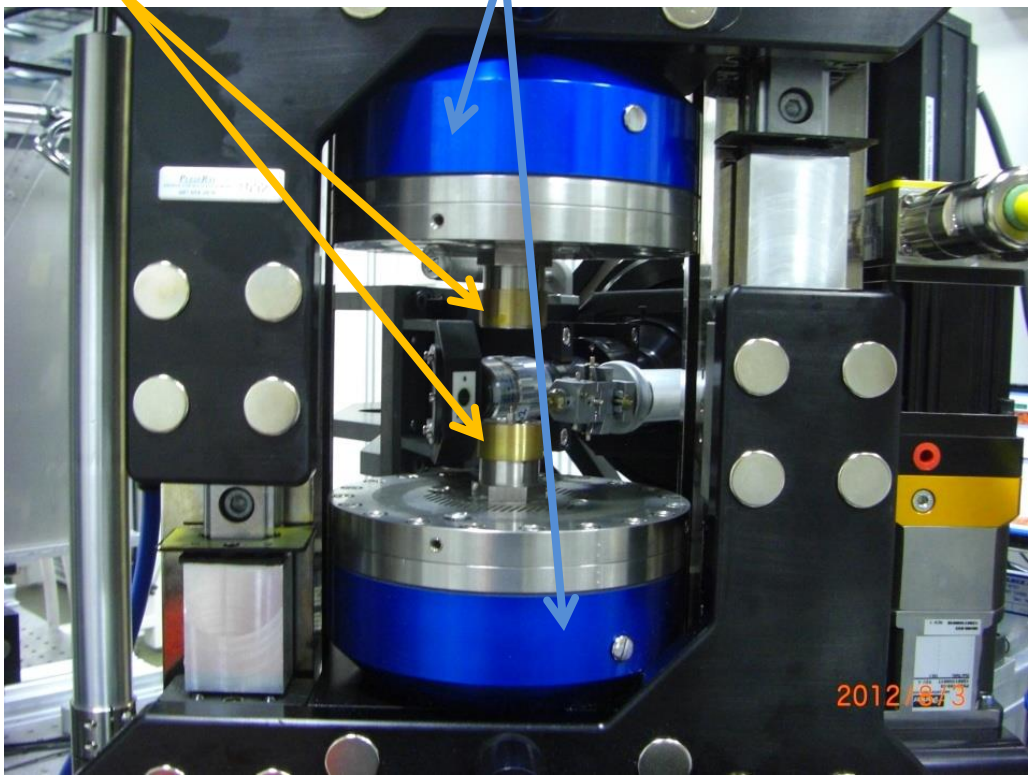

AFRL in-situ loading apparatus
Full rotation under load

Far Field Detector

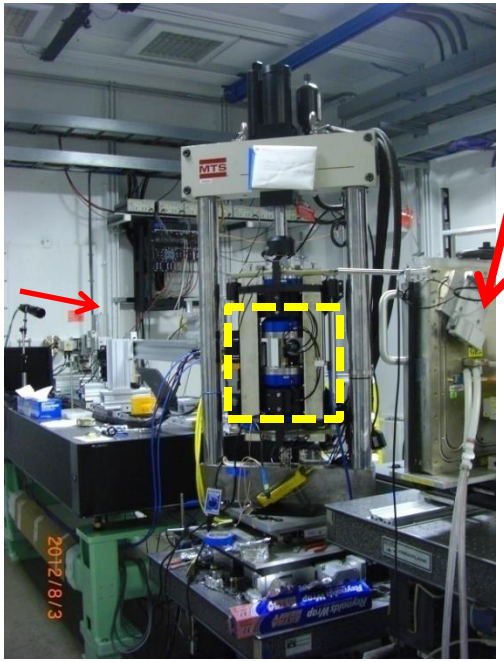

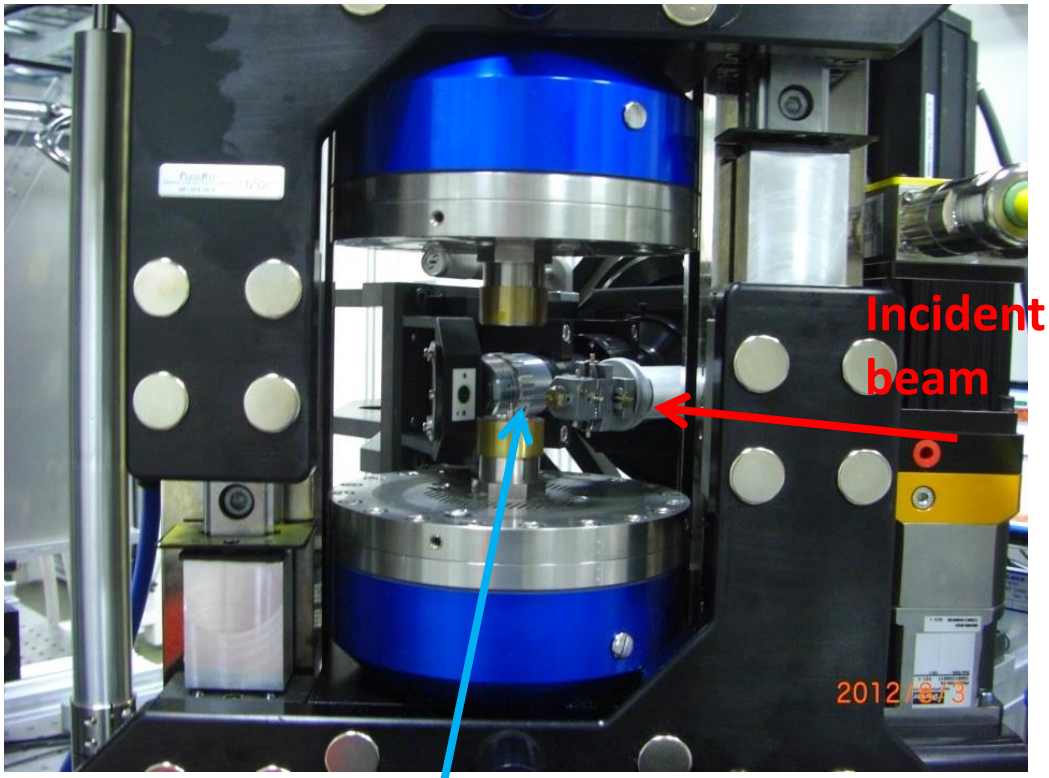

Beam block

AFRL in-situ loading apparatus
Full rotation under load

Near-field Camera

Far-field Detector

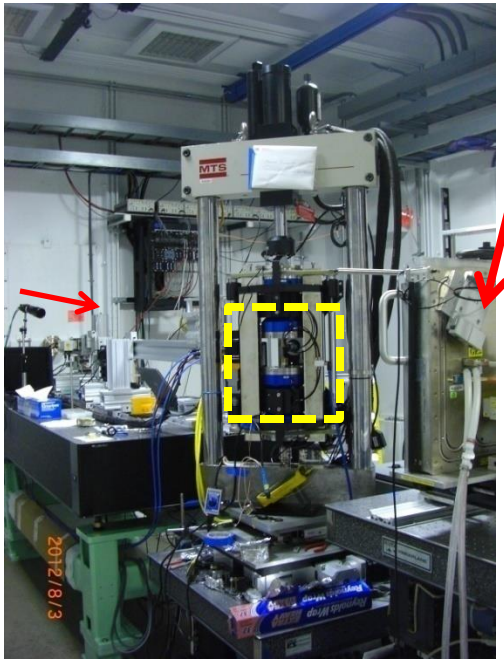

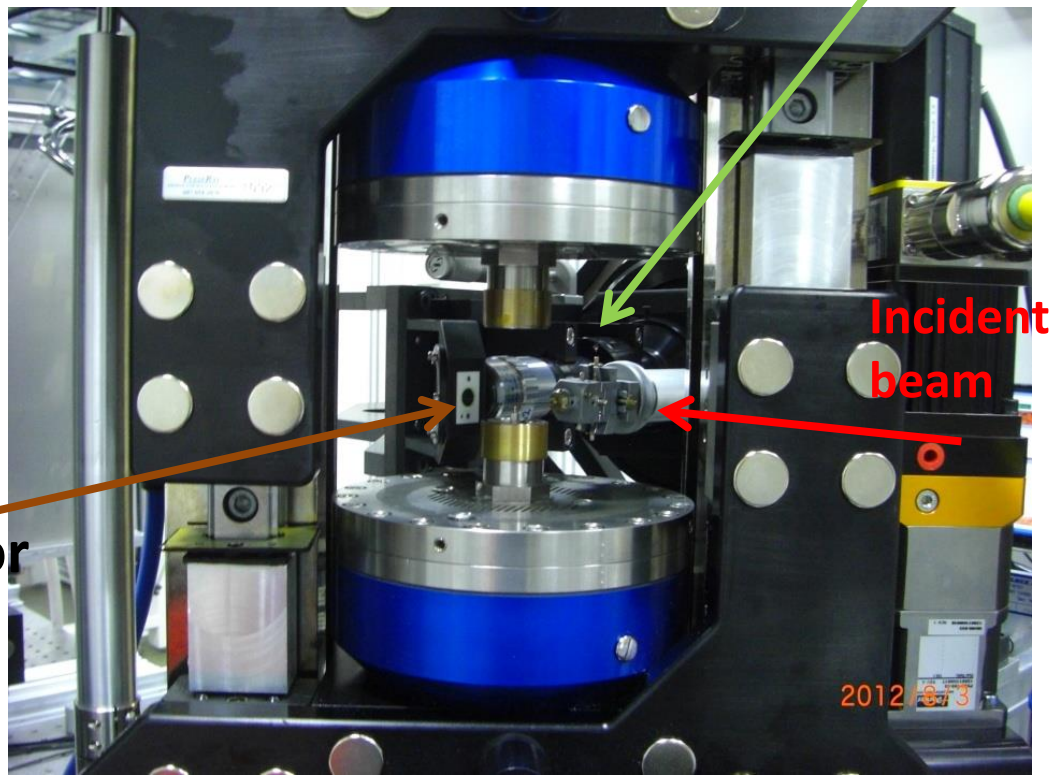

Incident beam

Scintillator

Observed Mesoscale Responses

Stress evolution under creep

AFRL/PUP team: in-situ combined nf- grain map & ff- strain tensors (in preparation)

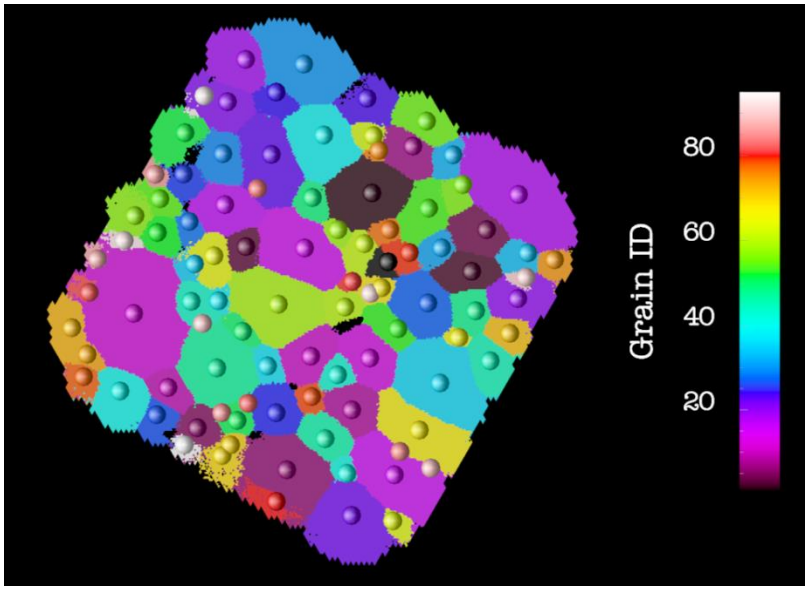

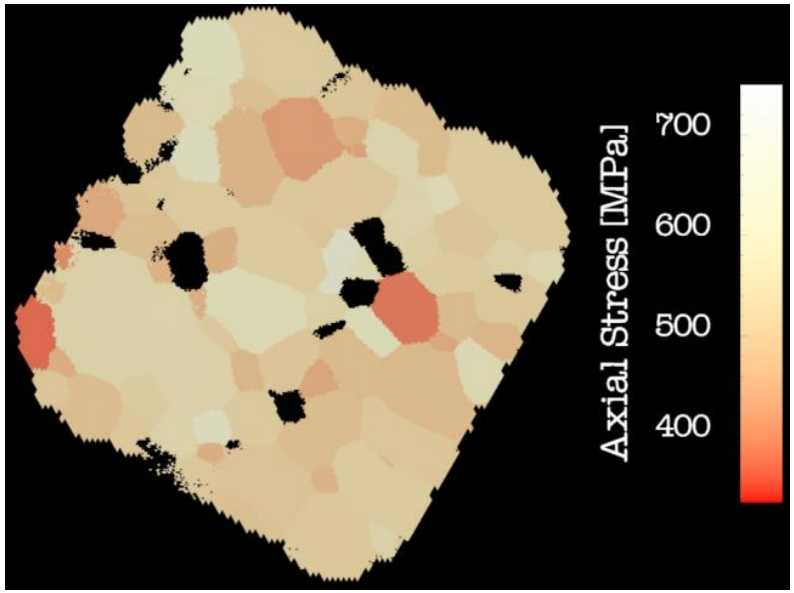

Ti-7Al

540 MPa
Post-creep

S. F. Li and J. Bernier computations

nf-, ff- & Tomography Combined

- **Thermally induced porosity**
  - **Overview:** TIP is thought to occur at grain boundary triple lines – using the full 3D dataset investigate coalescence statistics and the dependence on the local microstructure

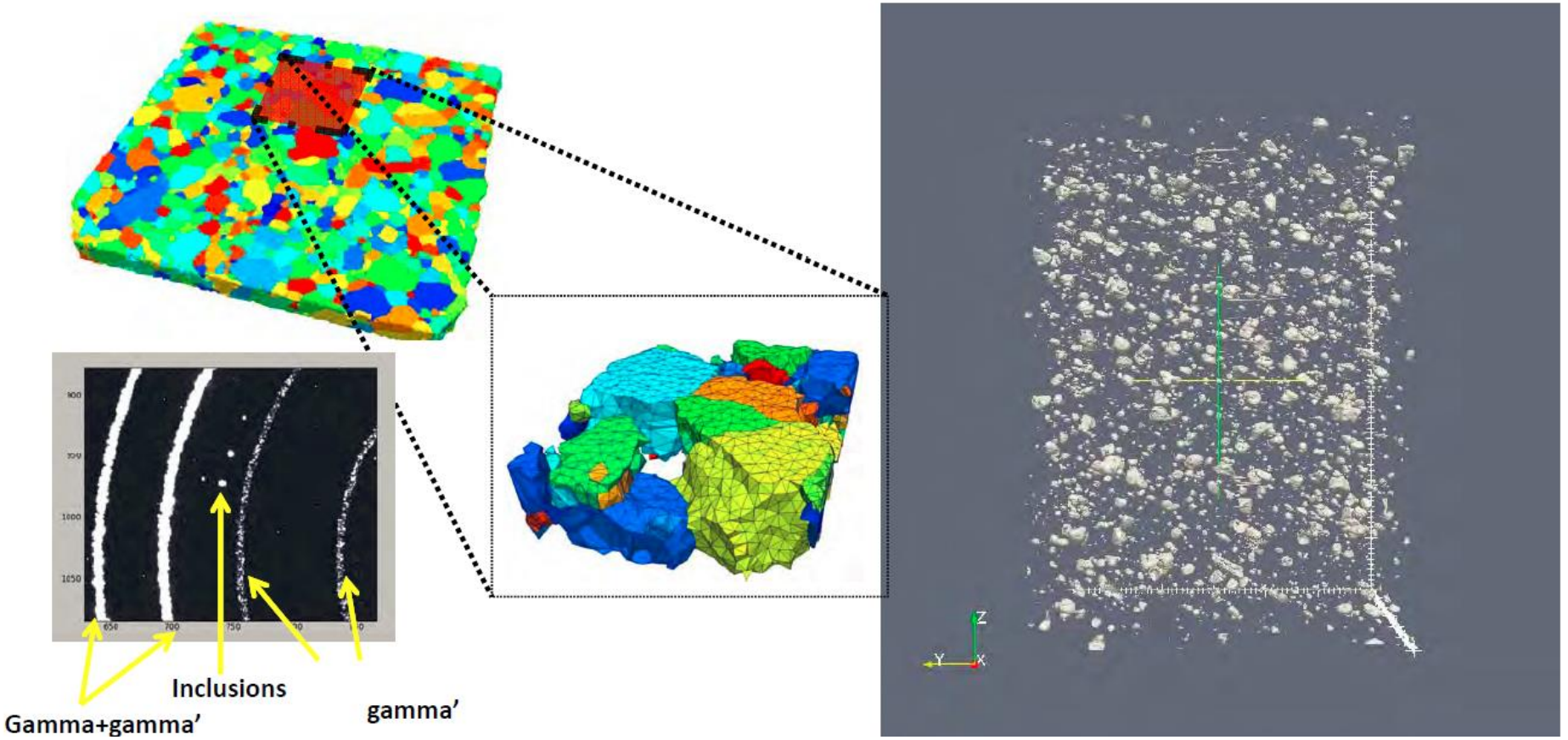

AFRL PUP team

Summary of Status

- Multi-modal HE X-rays probing polycrystal responses
  - In bulk, in 3D
  - Non-destructive
  - Thermal, fatigue, tensile, shock, irradiation,…
- Given nf- measurement, adding ff- is fast
  - Algorithms for coupled analysis
- Continued institutional investment
  - APS-U will make new modes practical and current ones fast/routine/better
  - AFRL PUP team: hardware, software, demonstrations
- Meso-scale characterizations tightly coupled to models:
  - X-rays provide unique tools for MGI, ICME concept

APS Upgrade

Towards a diffraction limited source

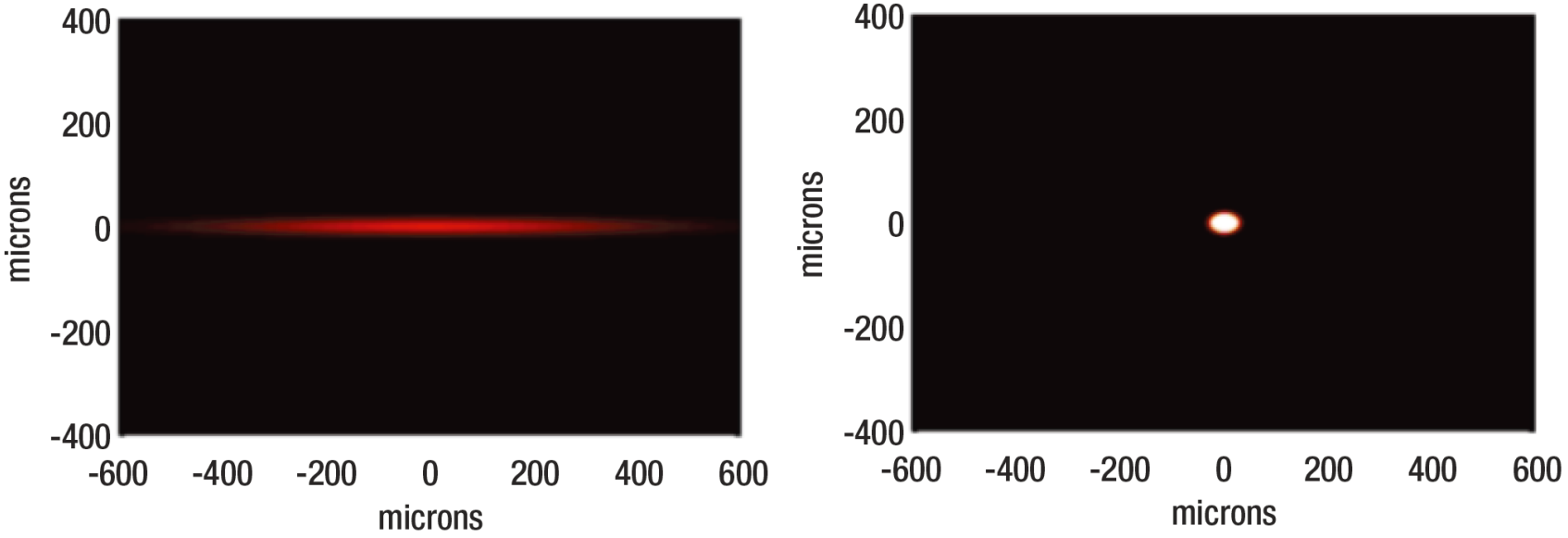

Computed beam profiles

Current APS

- **Vertical: close to diffraction limit**
- **Horizontal: ~25X diffraction limit**

MBA lattice at APS

- **Approximately symmetric**
- **Micron beam stability**
- **Superconducting undulator at Sector 1**